DESIGN AND CHARACTERIZATION OF A HOT-SURFACE IGNITION EXPERIMENT

A Thesis

by

DAVID SAMUEL TEITGE

Submitted to the Office of Graduate and Professional Studies of
Texas A&M University
in partial fulfillment of the requirements for the degree of

MASTER OF SCIENCE

Chair of Committee,	Eric Petersen
Committee Members,	Dion Antao
	Chad Mashuga
Head of Department,	Bryan Rassmussen

May 2021

Major Subject: Mechanical Engineering

ABSTRACT

The ignition of flammable liquids on hot surfaces is both a safety concern to industry and an important phenomenon for IC engines and some liquid propellant igniters. Hot-surface ignition is a function of fluid properties and environmental parameters, chiefly surface temperature. A new laboratory-scale experiment was constructed to determine the hot-surface ignition characteristics of flammable liquids without the presence of a spark. A stainless-steel block is heated using embedded electrical resistance heaters, and 20.5-μL drops of liquid fuel are dispensed onto removable test surfaces. Several experiment iterations with design improvements were implemented to minimize the negative effects of surface oxidation of the metal plate, droplet movement along the surface, and surface temperature non-uniformities. The final experimental apparatus is well-characterized, provides a uniform surface temperature within the range of 25-750 °C, and was utilized to characterize the hot-surface ignition of several flammable liquids.

Ten drops were tested at each surface temperature condition with a single test surface, which was replaced prior to testing alternative surface temperatures. This procedure was repeated at least once at each surface temperature, and the resultant datasets were reported as ignition probability (e.g., the percentage of ignition events per total number of drops at each temperature). These data were utilized to create ignition probability curves over a range of surface temperatures for all liquid fuels evaluated herein. The ignition probability data were also correlated with logistic regression curve fits. Furthermore, high-speed video analysis was completed to observe the fundamental phenomenon linked to hot-surface ignition. The experiment developed herein proved to be a useful tool for evaluating fundamental parameters that drive the hot-surface ignition behavior of various liquid fuels of interest.

DEDICATION

I would first like to thank Dr. Petersen who gave me the opportunity to work on all the incredible projects I have been a part of. I would also like to thank my committee: Dr. Antao and Dr. Mashuga.

Many thanks to my friends and colleagues who mentored and helped me along the way. I thank Dr. Chris Thomas in particular for the guidance and help at all hours of the day. He was an invaluable resource.

Finally, I would like to thank my family for their support and encouragement during my graduate studies. Your faith in me is well appreciated.

ACKNOWLEDGMENTS

The work herein was supported by the Texas A&M Experiment Station (TEES) through the Petersen Research Group and the TEES Turbomachinery Laboratory.

CONTRIBUTORS AND FUNDING SOURCES

Contributors

This work was supervised by a thesis committee consisting of Professor Eric Petersen [advisor] and Professor Dion Antao of the Department of Mechanical Engineering and Professor Chad Mashuga of the Department of Chemical Engineering.

The hot plate and heaters were designed and assembled by Dr. Chris Thomas and manufactured by Zachary Browne. The high-speed data analyzed in Chapter IV were collected with the help of Dr. Chris Thomas.

All other work conducted for the thesis was completed by the student independently.

Funding Sources

Graduate study was supported by a fellowship from Texas A&M University and a TEES Turbomachinery Laboratory Baker Risk Fellowship.

NOMENCLATURE

HSI	Hot-Surface Ignition
LTI	Lowest Temperature with Ignition
HTI	Highest Temperature without Ignition
SS	Stainless Steel

TABLE OF CONTENTS

LIST OF FIGURES

Page

LIST OF TABLES

Page

CHAPTER I

INTRODUCTION[*]

Motivation

The ignition of flammable liquids on hot surfaces without the presence of a spark or flame is a safety concern for some industries but also a potential ignition method in some liquid engines and propellant igniters. The phenomenon is commonly termed hot-surface ignition (HSI) and is a probabilistic event. HSI is affected by the flammable fluid's thermophysical properties (specific heat, heat of vaporization, activation energy, etc.) and is dependent on environmental parameters such as air currents over the hot surface [1,2]; surface material [1,3]; geometry/size [1,3,4]; roughness/cleanliness [5-7]; surface temperature; liquid drop height/velocity [3,8]; and volume [3,6,7]. It is generally accepted that the most significant factor affecting HSI is the surface temperature but determining the influence of other factors on the ignition probability is crucial to applying laboratory-based experimental data to realistic environments in a predictive manner.

There is not currently an established standard test method that directly applies to HSI. ASTM E659, Standard Test Method for Autoignition Temperature (AIT) of Chemicals [9], is the closest analog to HSI, but AIT values can be anywhere from 50-450 °C below the HSI threshold [6,8,10,11]. Furthermore, section 5.3 of ASTM E659 states that it is not designed for liquids that undergo exothermic decomposition (below their ignition temperature) which is the case for many hydrocarbon fuels and oils. Alternative standard experiments such as ASTM D4206 [12], D92 [13], or D1310 [14] can be utilized to determine the flash point or fire point of a substance by bringing an external flame into contact with it at different temperatures. However, the external

[*] Reprinted with permission from "High-Speed Video Analysis of Lubricating Oils Undergoing Hot-Surface Ignition" by David S. Teitge, James C. Thomas, and Eric L. Petersen, 2020. AIAA Propulsion and Energy Forum, Copyright 2020 by the authors.

flame is not generally present in HSI, so the flash point or fire point of a liquid should not be treated as representative of HSI temperatures. However, it is worth noting that some researchers [10] have observed a possible correlation between HSI temperatures and flash point.

The combination of a lack of available standard experiments and the wide range of environmental parameters in HSI generally forces a safety engineer to develop and conduct their own HSI experiments. The available literature contains a wide variety of experiments characterizing HSI for some common fuels tested under a range of environments. For the present work, the authors were motivated to design and characterize an in-house HSI experiment that was tailored for studying the HSI probability of gas turbine lubricating oils, kerosene-based fuels, and rocket propellants, with and without various additives.

Arrangement of Thesis

In the following section, an in-depth look into the available literature is discussed with a focus placed on experimental setup and procedures. The design iterations for the current experiment are detailed at the end of Chapter II. Chapter III describes a heat transfer model that was built to analyze uncertainties in experimental measurements and to perform quick studies on thermal properties. In Chapter IV, high-speed video stills are used to determine necessary design improvements and to observe fundamental evaporation and ignition phenomenon. Chapter V presents ignition probability data collected with the experiment and makes comparisons to data in literature. Finally, Chapter VI provides conclusions and future work for this experiment.

CHAPTER II

BACKGROUND[*]

Literature Review

A summary of some key experimental testing parameters from HSI experiments detailed in the literature and from the current study is provided in Table 1. The wide range of parameters that were varied among research efforts potentially accounts for the disparities in HSI probability data provided for seemingly similar fuels. Unfortunately, HSI experiments were not always fully characterized in the literature, so discerning the influence of various parameters on the corresponding data can often be difficult. The available literature on HSI experiments is detailed, as follows.

The catalytic nature of the surface metal was first observed in HSI tests using gaseous methane. Coward and Guest [15] determined that higher temperatures (150-375 °C) were necessary to ignite a methane mixture on platinum compared to stainless steel (SS). It was also noted that as mixtures neared stoichiometric conditions, higher temperatures were required for ignition. The platinum surfaces glowed red hot several minutes after heat input was terminated, indicating an ongoing reaction. The team concluded that the catalytic nature of the surface caused radicals to be consumed so quickly at the surface that the reaction zone could not expand despite the high temperature. This effect could be increased or decreased by treating the surface with a greater level of catalysts or catalytic poisons, respectively. Although this example does not directly involve the evaporation of a liquid, it does illustrate the effects of the surface composition on apparent HSI.

[*] Reprinted with permission from "Hot Surface Ignition Probability of Hydrocarbon Fuels and Oils" by David S. Teitge, James C. Thomas, Thomas E. Sammet, Zachary K. Browne, and Eric L. Petersen, 2020. Central States Section of The Combustion Institute.

Table 1: Summary of key parameters in experimental setups as seen in the literature. Reprinted with permission from [16]

Group	Fluid Type	Surface Material	Drop/Spray	Volume (µL)	Drop Height (cm)	Temperatures (°C)	Surface Cleaning	Enclosedness
Colwell and Reza [5]	automotive	304 SS	drop	20-34.1	25	450-750	sanded	3 walls
Davis et al. [6]	automotive	304 SS	spray	250	n/a	430-825	steel wool, ethanol	none
Goyal et al. [8]	aviation	304 SS	drop	25	25,30	670-810	n/a	none
Ebersole et al. [7]	automotive	cast iron	spray	10,000	n/a	640-820	sand blasted	moderate
Byers et al. [3]	automotive	Stainless/ austenic/ferritic steel, cast iron	drop	9.3	2.5	400-675	n/a	none
Demetri and White [4]	automotive	nichrome foil	atomized spray	n/a	8.89	890-1090	n/a	complete
Myronuk [1]	aviation	304 SS, 321 SS, 1040 carbon steel, aluminum, chrome alloy, titanium alloy, Inconel, molybdenum	atomized spray	~15,000	n/a	325-925	n/a	none
Current Study	turbine oil, liquid monopropellant	316 SS, titanium alloy	drop	20.5	4.5	500-750	acetone, sandpaper	3 wall

According to research from Tanabe and Imoto [17], the oxidation of 316 SS (and presumably other steels) increases greatly at temperatures above 600 °C because metal and oxygen ions begin to diffuse more easily through the oxide layer. They note that the relative concentration of metals in 316 SS differs from that seen in the oxide layer, which might lead to a difference in catalytic performance of the surface. Polished samples exhibited exfoliated oxide layers, which have greatly increased surface roughness. Since most HSI tests occur on SS surfaces, these oxidation effects should be seen across experiments.

Myronuk [1] primarily tested aviation fuels and hydraulic fluids on austenitic SS (type 321) and titanium B265-58T but included notes on experiments with Inconel X750 and molybdenum (common metals used in the aviation industry). The heated surface area was 7.62 cm × 1 m and included complex conditions such as forced air flow (0-50 m/s) with stagnation zones created by surface obstacles. High air velocities increased ignition delay times and severely lowered HSI probability for more-volatile fuels. Ignition became independent of air velocity however above 850 °C for most fuels. Anti-misting additives included in JP-5 served to lower the lowest temperature with ignition (LTI) by 10-50 °C. Myronuk [1] also remarked that catalytic agents such as carbon and metallic oxides present on the SS surface lowered ignition temperatures by 50-75 °C when compared to titanium. It was also noted that the oxide formed on molybdenum lowered the LTI but was consumed in the combustion and replaced by a yellow trioxide which ultimately increased the LTI beyond what was observed for SS.

Demetri and White [4] tested liquid and vapor fuels to determine ignition delay time and ignition temperature. For their liquid experiments, an atomized spray fell onto strips of variable-width nichrome sheets. The volume dispensed was not reported, but the experiment was reported to produce droplets with diameters of 60-110 microns and an equivalence ratio of one assuming

the vapors filled the entire reactor, although it is noted the ratio was obviously higher near the hot surface. Surface temperatures were monitored with an NPN (Negative-Positive-Negative) Planar Silicon Phototransistor that was sensitive to infrared (IR) and calibrated to a thermocouple. A model for ignition delay time was developed which assumed vaporization, mixing, and reaction occur sequentially rather than simultaneously. Although this sequential behavior seems unlikely, relatively good agreement between the model and data was observed. In the vaporized portion of the study, it was noted that thermal ignition was insensitive to concentration for a given fuel and surface size. This concentration insensitivity may be attributed to a lack of catalytic action on the nichrome surface. It is also worth noting that decreasing the heated area by a factor of four raised the LTI by 60 °C for a given fuel.

Bennett [18] investigated the surface effects on HSI and proposed a geometric surface modification to reduce heat flux, and thus HSI probability. Bennet [18] stated that because of fluid properties, surface roughness could either promote or inhibit vaporization and/or ignition delay times. This effect is because, although increased roughness increases the surface area, it could also decrease the contact area with the fluid. Bennet [18] also stated the importance of boiling regimes by correlating LTI reported by other research groups to the boiling regimes for the fuel at that temperature.

Colwell et al. [5] implemented a simple experiment which released a single liquid droplet onto a heated surface surrounded by walls on three sides to block air currents. Droplet volume was not well regulated but was instead computed as the total volume dispensed divided by the number of droplets. The surface was sanded before testing of new fluids to remove any potential residue. A logistic regression curve was fit to the ignition data to determine ignition probability as a function of temperature, and a chi-square goodness-of-fit test was used to confirm the quality of

the fit. The highest temperature with no ignition (HTI) and the LTI were also reported for each fuel. Figure 1 has been adapted from Colwell et al. [5] and shows the relation between the ASTM standard experiments and HSI experiments as well as the relative temperatures necessary for each.

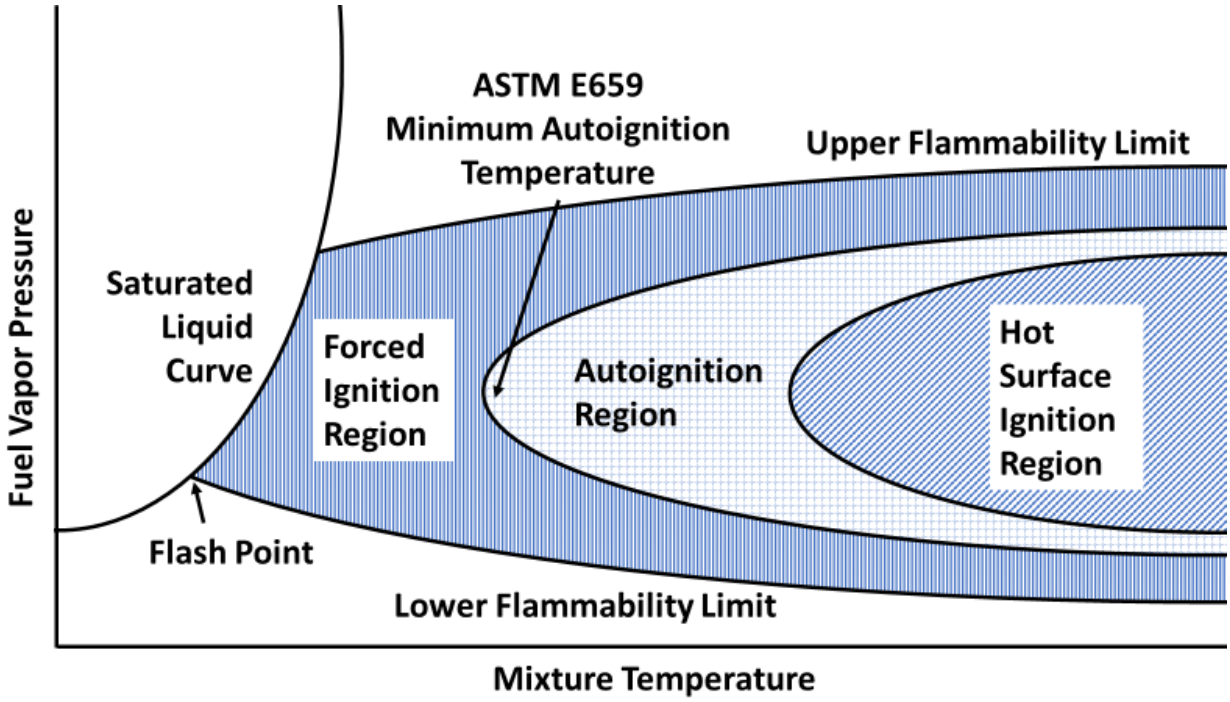

Figure 1. Ignition regions as functions of fuel vapor pressure and mixture temperature. This has been adapted from Colwell et al. [5]. Higher temperatures are necessary for HSI compared to AIT, but it is unknown if fuel vapor pressures necessary for ignition differ. Reprinted with permission from [19].

Groups from Exponent, Inc. have conducted several HSI studies with automotive fluids. Davis et al. [10] sprayed 250 µL of various fuels onto a hot surface made of 304 SS. One key finding was that the HSI probability is dependent on fluid volume. They also determined that volatility, boiling point, and octane number played minor roles in predicting HSI temperature, whereas a linear correlation was observed between AIT and HSI temperatures for some fuels. Somandepalli et al. [11] tested ethanol-blended fuels and biodiesel on the same experimental setup as Davis et al. [10]. It is worth noting that the LTI of one fuel recorded by Somandepalli et al. [11]

differed from the LTI reported by Davis et al. [10] by approximately 100 °C despite using the same experimental setup. This disparity is presumably derived from some minor differences in the fuel tested. In general, the ethanol-blended fuels had lower LTI than their counterparts without ethanol, as expected. Davis et al. [6] further evaluated various high-performance motorsport fuels. Their procedure included covering the surface in between sprays and cleaning the surface with steel wool and ethanol between experiments. They found no clear relationship between octane number and LTI, as previously hypothesized [10].

Probably the most thorough investigation to date was performed by Byers et al. [3]. They tested 9.32-µL drops of standard 87 Octane gasoline on 304 SS, cast iron, austenitic steel, and a coated ferritic SS. They reported temperature data collected from both a thermocouple and from IR thermography for each of the four surface materials. It was noted that the thermocouple on the hot surface seemed to increase ignition probability when the droplet touched it, possibly due to increased heat flux into the fluid. The drop height in this experiment was 2.54 cm, and at least 8 data points were collected per temperature, likely because data points where droplets touched the thermocouple were not kept. The exposed surface area was small (3.1 cm diameter), although a noticeable temperature gradient existed. To account for this gradient, an average temperature of six locations on the surface was reported for each test. Regardless, Byers et al. [3] reported data for gasoline on 304 SS that were in good agreement, though slightly lower, with three other experiments in the literature. This slightly lower probability is of interest considering Byers et al. [3] used much smaller fuel droplets than the other three experiments. This result may indicate that liquid volume has less of an impact on ignition than hot surface area and/or drop height (which ultimately affects the temperature of the fuel before it touches the surface). It may also indicate that surface area and liquid volume can be lumped together into one single parameter when

comparing data amongst various experimental configurations. Their experiment also confirmed the effect of metal composition on surface ignition, as well as the effect of surface cleanliness on ignition. More explicitly, higher surface temperatures were necessary to ignite the same fuel the longer the cast iron sample was utilized for testing without cleaning or sanding.

Babrauskas [2] suggested that the most important variable among the parameters is the "degree of enclosedness." Indeed, this factor is significant since it ultimately impacts the fuel-air ratios above the hot surface as the fuel evaporates prior to the ignition event. Accordingly, as a system becomes more enclosed, HSI events should behave like AIT experiments.

Ebersole et al. [7] made crucibles from cast iron and heated them with hot plates in a fume hood. The crucibles were either sand blasted or Roto-Blasted after ten data readings. A constant stream of liquid was sprayed into the crucible at a rate of roughly 2 mL/s for up to a total volume of 10 mL. The large volume of liquid noticeably cooled the surface upon contact, but lower LTI were still noted. This observation suggests larger pools of liquid may be more prone to HSI ignition. The data collected by Ebersole et al. [7] contained a significant amount of scatter, potentially because only 10 tests were completed at each temperature. The results indicated that HSI temperatures decreased with increasing ethanol content whereas AIT remained relatively constant.

Goyal et al. [8] dropped 25 µL of common aviation fuels onto a heated 304 SS surface. Variation of the drop height (25 or 30 cm) illustrated a minor effect on the HSI probability. They remark that most prior studies used heights between 15 and 30 cm. As seen in Fig. 2, there is much greater scatter in the data from Ebersole et al. [7] when compared to the data from Goyal et al. [8], probably due in part to the number of tests done at each temperature. No decrease in ignition probability with higher temperature is reported by Goyal et al. [8] although it does flatten out

around 80% over roughly 10 °C. The fuel types differ between groups (Goyal et al. [8]: Heptane, Ebersole et al. [7]: Indolene), but the high level of scatter in the Ebersole et al. [7] data is not seen in any other data reported in literature.

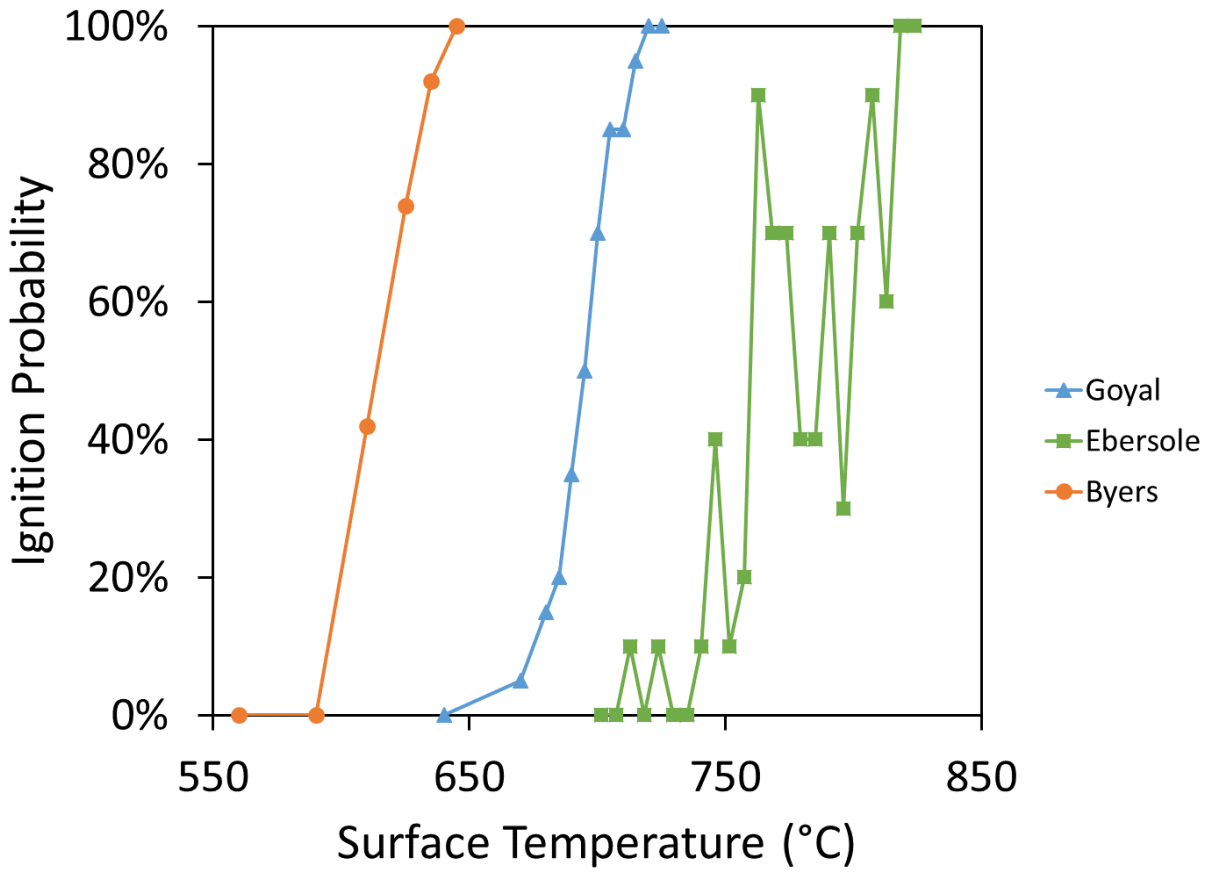

Figure 2: Comparison of data from literature. Data shown was collected by Ebersole et al. [7] who collected 8 data points per temperature, Goyal et al. [8] who collected 20 data points per temperature, and Byers et al. [3] who collected at least 8 data points per temperature with standard 87 octane gasoline. Reprinted with permission from [16].

In summary, environmental parameters that can influence HSI include air currents over the hot surface; surface material; geometry/size; roughness/cleanliness; surface temperature; liquid drop height/velocity; and volume. Surface temperature has the greatest impact among these, while the others ultimately affect droplet/vapor temperatures, fuel-air ratios, or surface catalytic effects.

Some studies chose to focus on liquid dwell time or ignition delay time, but a change in these values may cause higher or lower LTI depending on the fuel's thermophysical properties. Some attempts have been made to correlate HSI to other temperatures such as AIT, flash point, or fire point, but so far these correlations are limited to specific types of fuels. Further studies are necessary to fundamentally understand HSI events.

Design Improvements

An image and schematic of the first-generation experimental setup at Texas A&M University are shown in Figs. 3 and 4, respectively. Three cartridge heaters with internally embedded thermocouples were sealed inside of a 304 SS plate with high thermal conductivity paste (AREMCO silver-filled conductive paste, 597-C). The cartridge heaters are individually controlled by 3 PID controllers and can reach temperatures as high as 750 °C (1382 °F). The SS block is surrounded on 4 of its 6 faces by insulation to protect the fume hood it is contained within and to minimize heat losses. A scientific pipette is utilized to dispense liquid droplets with volumes ranging from 0 to 20.7 μL. The pipette is held in a burette stand that allows for variation of the droplet height. The height was set herein such that the liquid droplet did not break up on impact with the surface (~10 cm at this time). A calibration curve was produced that correlated the surface temperature (measured using a thermocouple probe at the test location) to the internal temperature of the cartridge heaters.

Prior to testing, the SS block's core temperature was set to the desired value and given enough time for the surface to reach steady-state temperature. A 20.5-μL droplet of the selected fuel was released from the pipette and fell to the hot surface where it evaporated and may or may not have ignited. Two minutes were allotted between testing of additional droplets to allow the surface to reach steady state temperature once again. A total of 20 data points was recorded at each

temperature of interest for each fuel. The ignition probability of each fuel at a given surface temperature is computed as the total number of ignition events divided by the total number of trials.

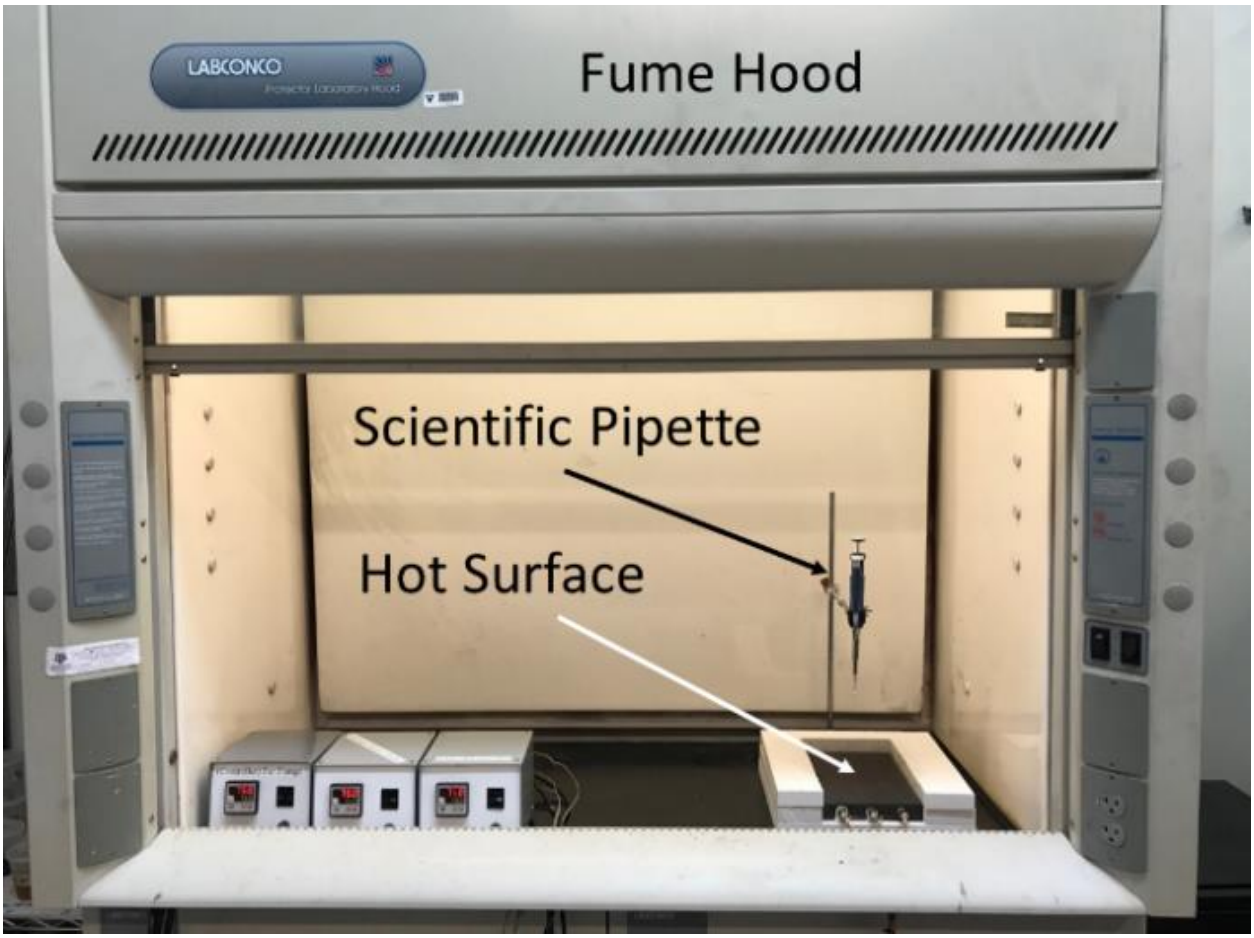

Figure 3. Early experimental setup for ignition of fuels and oils. The hot surface consists of a 304 SS block with three internally embedded cartridge heaters which contain internal thermocouples. Reprinted with permission from [16].

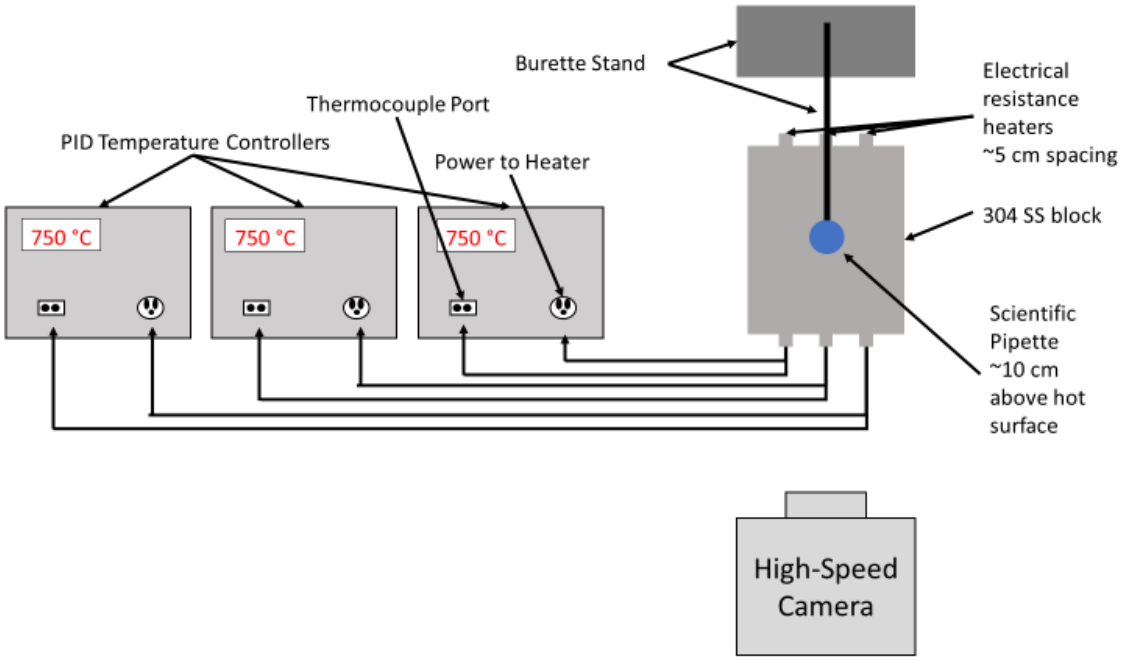

Figure 4. Schematic view of first-generation experiment. Shown above is a schematic of the key connections and locations of components used in this experiment. Key diagnostics include PID temperature controllers, internal thermocouples, and a high-speed video camera. Reprinted with permission from [19].

Repeating the test for one fuel at one core/surface temperature over the course of a few weeks made it clear that the data were not consistent and repeatable, at least for the first-generation procedures. More explicitly, ignition probability at some temperature was steadily decreasing as the experiment was being used. The authors determined this aging effect was due to the metal oxide layer forming at the hot surface, as has been previously described by other researchers. Accordingly, more control over the ignition surface (oxide layer thickness, cleanliness, etc.) was necessary for consistent measurements. Furthermore, the authors noted that droplet motion after impact with the hot surface was seemingly random, exposing the droplet to a potential temperature gradient on the hot surface.

To overcome these challenges, the second-generation experimental procedures were developed and included utilization of thin sheet metal and washers (shown in Fig. 5) that were

placed atop the hot surface. Both the sheet metal and the washers were made of 316 SS, which was selected for its high-temperature, corrosion-resistant properties. The sheet metal was purchased in long strips of 152.4-µm (6-mil) thickness which were cut using a circular die to produce 2.54-cm (1-inch) diameter pieces. The washer was incorporated to keep the round sheet metal in place during testing and to prevent the fuel droplet from leaving the sheet metal surface. This method produced good repeatability (shown in Fig. 6) when 20 data points were collected per temperature. Oxidation still occurs on the sheet metal pieces, but this layer is not as developed as the layer on the 304 SS block and was visually consistent across test pieces. The inexpensive test pieces were discarded after each test, but the washers were cleaned in acetone in between tests.

Figure 5. Second generation test surfaces. These are made from cut SS sheet metal and SS washers. Reprinted with permission from [16].

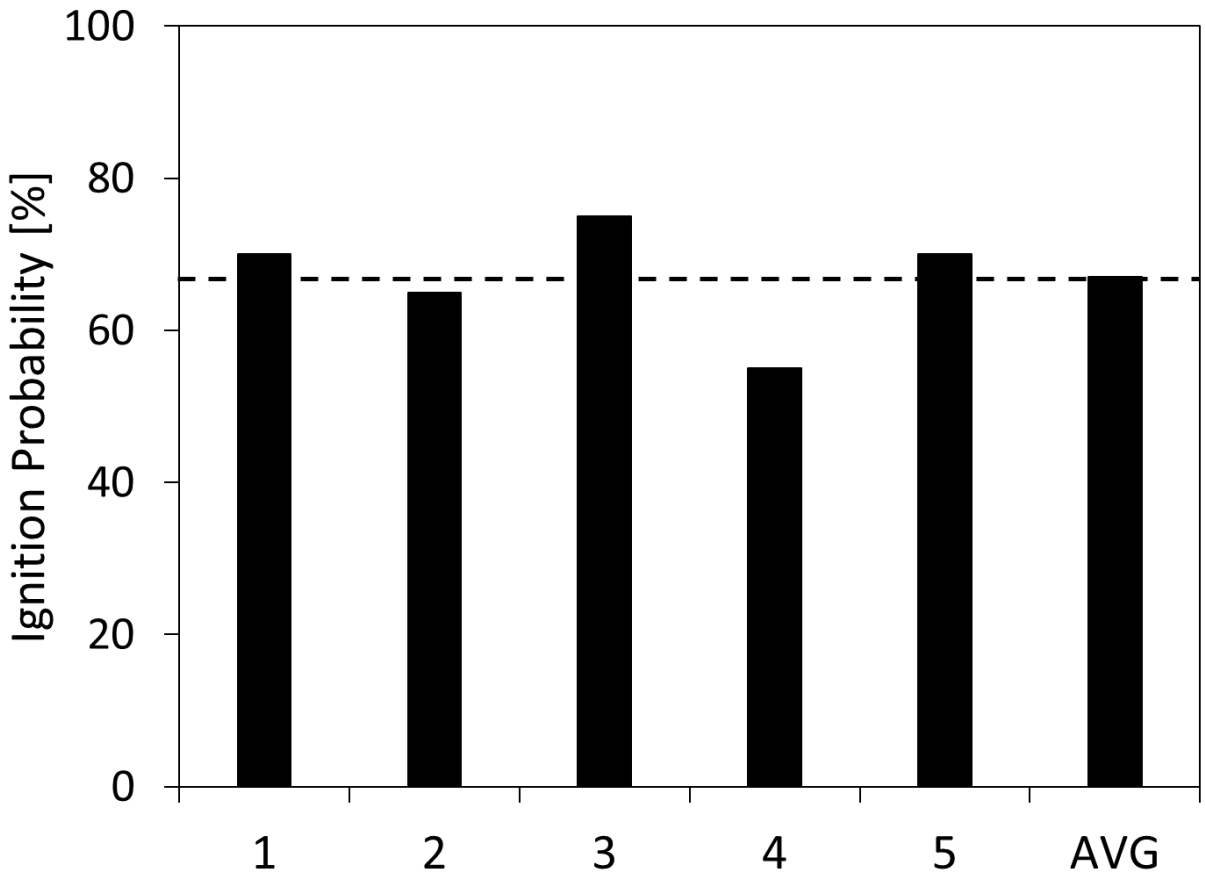

Figure 6. Second generation demonstration of repeatability. Shown above is the ignition probability for one test condition as determined with the removable test pieces shown in Fig. 5. Reprinted with permission from [16].

The disposable test pieces were convenient and quick, but liquid droplet contact with the washer had the potential to increase the heat flux into the droplet which could affect results. Accordingly, a more robust reusable test surface was implemented (Fig. 8). The removable test surface is placed into a recess in the block's surface (as can be seen in Fig. 9) to ensure consistent placement and improve heat conduction. The top of the test surface was given a slight bowl shape to constrain droplet motion, thus reducing the effects of temperature gradients on the surface and improving video capture capabilities.

An additional layer of insulation was added to the top surface to add control of the exposed surface area and improve the temperature capabilities of the experiment by reducing radiative heat losses. The area of the exposed surface is an important factor since it determines the temperature and convection current behavior in the region. The first hole size implemented was 2.54 cm (1 in) to match the size of the test surface. No ignition was observed for a relevant oil (Mobil DTE 732) in this condition, even at the maximum temperature capability of the experiment. This finding was potentially due to a lack of air flow to the fuel rich region, so the insulation was machined thinner around the test piece opening while still only exposing the 2.54 cm dimeter region of the test surface. However, ignition still did not occur in this configuration. Accordingly, a 10.16-cm (4-in) hole was cut in a new piece of insulation and placed on top of the surface. This configuration did allow for ignition when dropping a 20.5-µL drop of the fluid onto the removable test surface from a height of 4.5 cm. These observations potentially suggest the existence of a minimum exposed surface area required for HSI to occur. Furthermore, it is probable that the ratio of fluid surface volume to heated surface area must overcome some limit for the hot surface to add enough energy to the fluid for ignition. More knowledge of this relationship would inform an even better-designed HSI experiment in the future.

A K-type thermocouple is embedded just beneath the center of the test surface to actively monitor the sub-surface temperature during tests. The test surface is only 0.5 mm (0.02 in) thick at the center, so the embedded temperature is very close to the surface temperature. An infrared temperature gun was utilized to measure the ‘true’ surface temperature for comparison to the sub-surface temperature measured by the embedded thermocouple. A small temperature drop across the test surface was observed (Fig. 7), which increased with increasing temperature. The two

temperature measurements are well correlated with a linear approximation, which now serves as the calibration curve for all experiments conducted herein.

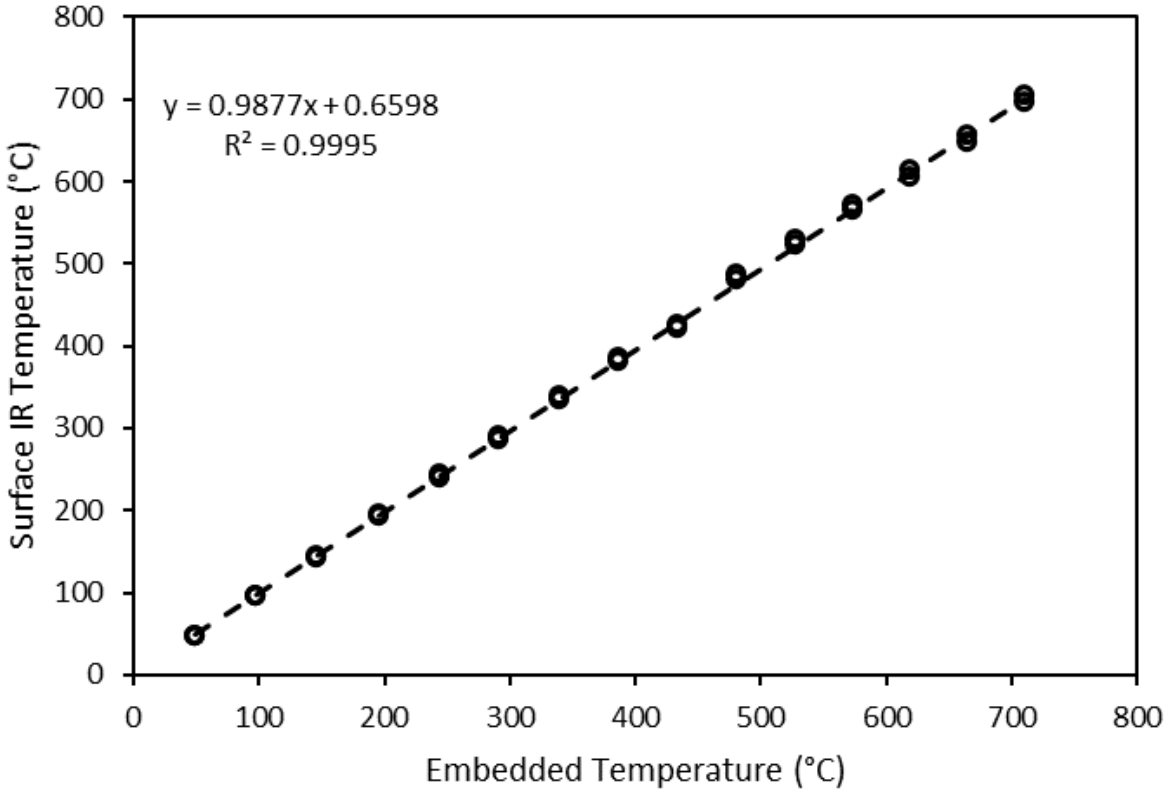

Figure 7. Relationship between the embedded temperature and the surface temperature. The embedded temperature is recorded by a thermocouple beneath the center of the test surface. The surface temperature is recorded with an IR temperature gun. An emissivity of 0.815 was used for the metal surface after calibration with the embedded thermocouple.

Air barriers were added to the sides of the experiment after looking at high-speed video, which is mentioned in Chapter IV. It was noticed that the flames tended to be blown to the left of the test surface, suggesting an air current inside the fume hood. These side air barriers (Fig. 9) prevent these air currents from blowing across the surface, thus maintaining a quiescent environment. A front barrier was used during high speed video tests to protect the camera lens

from the heat and to block air currents in the room from blowing into the fume hood. With these barriers, the surface is isolated from forced convection flows.

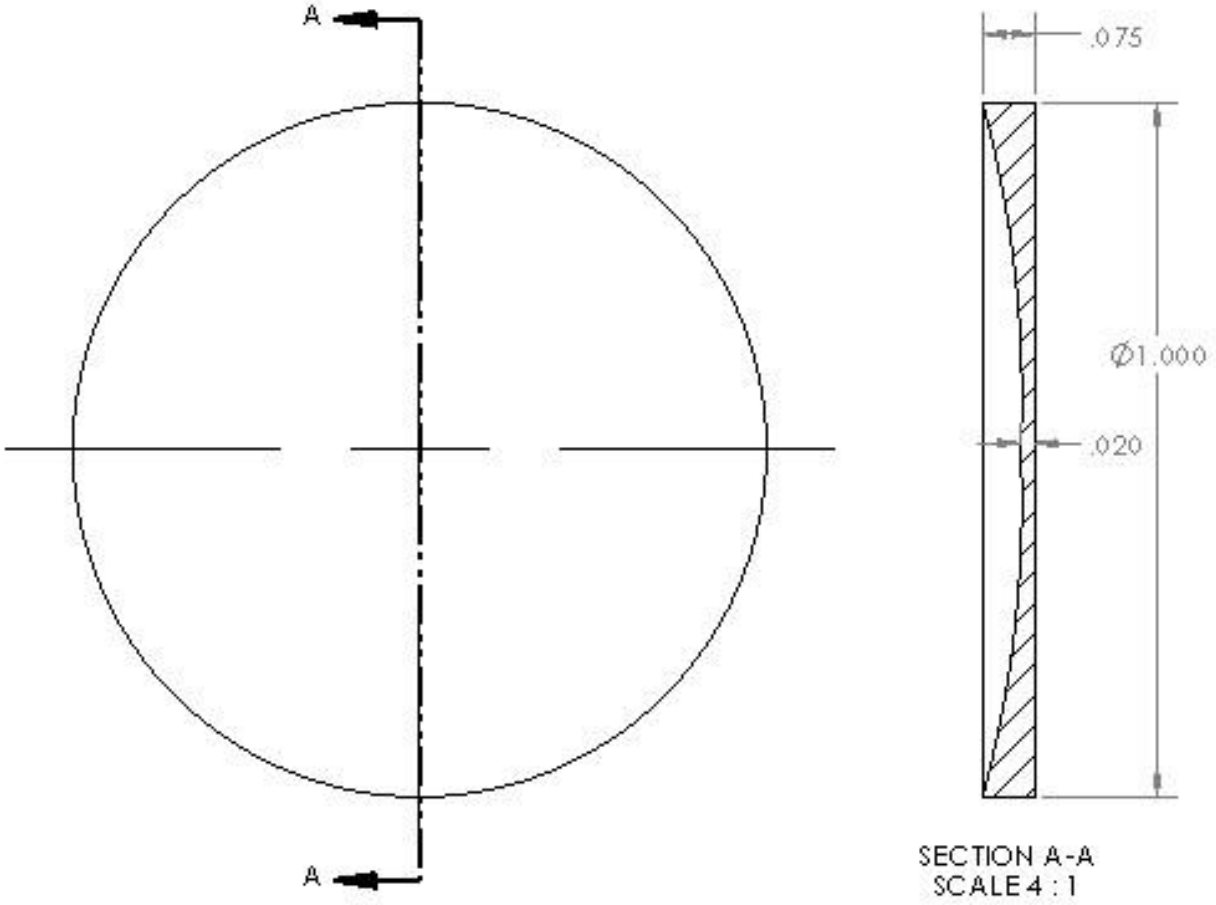

Figure 8. Dimensioned drawing of the reusable test surfaces. The 316 SS pieces were made as thin as possible to reduce temperature drop across the surface.

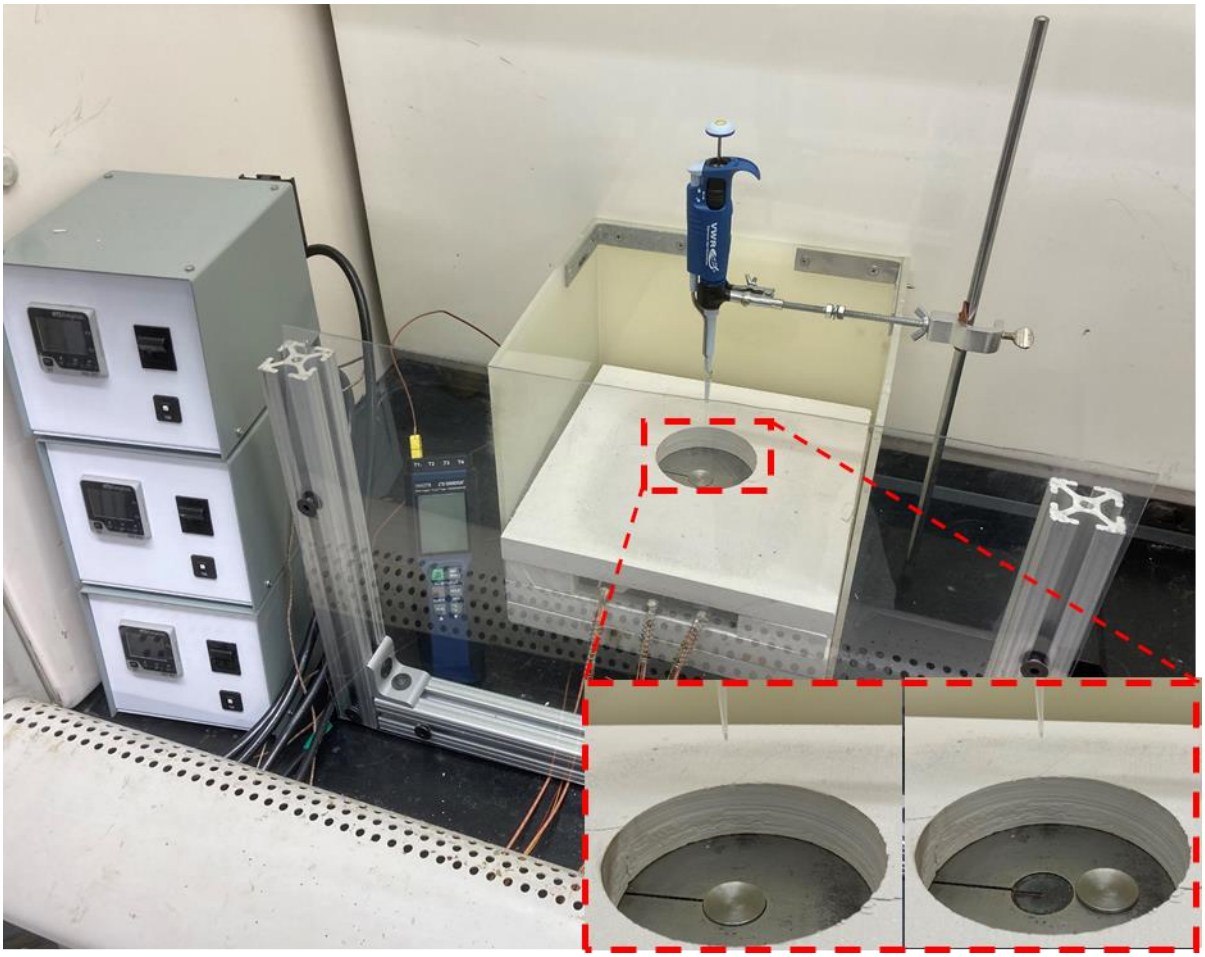

Figure 9. Third generation experimental setup. This configuration uses 3 walls around the experiment and a transparent shield in the front to block air currents from the room. The image inserts in the bottom-left depict the recess where the test surface rests during testing.

CHAPTER III

HEAT TRANSFER MODEL

A one-dimensional, steady-state heat transfer model was developed to improve understanding of the experiment and to validate assumptions implemented within experimental trials. A schematic representation of the model is shown in Fig. 10 which depicts a steady-state heat transfer rate from the middle, embedded resistance heater to the SS block and to the test surface. A thermal circuit is shown in Fig. 10 which consists of conductive and contact insulance terms. The values of key dimensions are: t=0.156 in, d=0.196 in, and h=0.02 in. The heater casing and SS block are both made of SS 304, and the test surfaces utilized herein are made of SS 316. One key assumption made within the modeling framework is that the contact resistance between the embedded heater and SS block is negligible due to the presence of the highly conductive thermal paste. The steady-state heat transfer rate through the system can be written as:

$$\dot{Q}_{SS}^{"} = \frac{T_{s,1}-T_{s,2}}{\emptyset_{12}} = \frac{T_{s,2}-T_{s,3}}{\emptyset_{23}} \tag{1}$$

where $\emptyset_{12}$ and $\emptyset_{23}$ are thermal insulance terms described by:

$$\emptyset_{12} = \left(\frac{t}{k_1}\right) + \left(\frac{d}{k_2}\right) \tag{2}$$

$$\emptyset_{23} = R_{c,2} + \left(\frac{h}{k_3}\right) \tag{3}$$

The experiment can cover a wide range of temperatures, such that temperature-dependent thermal conductivities are required for accurate modeling. Accordingly, relations presented by Valencia et al. [20] are implemented within the modeling framework:

$$k_{304SS} = 10.33 + (15.4 \times 10^{-3})T - (7.0 \times 10^{-7})T^2 \tag{4}$$

$$k_{316SS} = 6.31 + (27.2 \times 10^{-3})T - (7.0 \times 10^{-6})T^2 \tag{5}$$

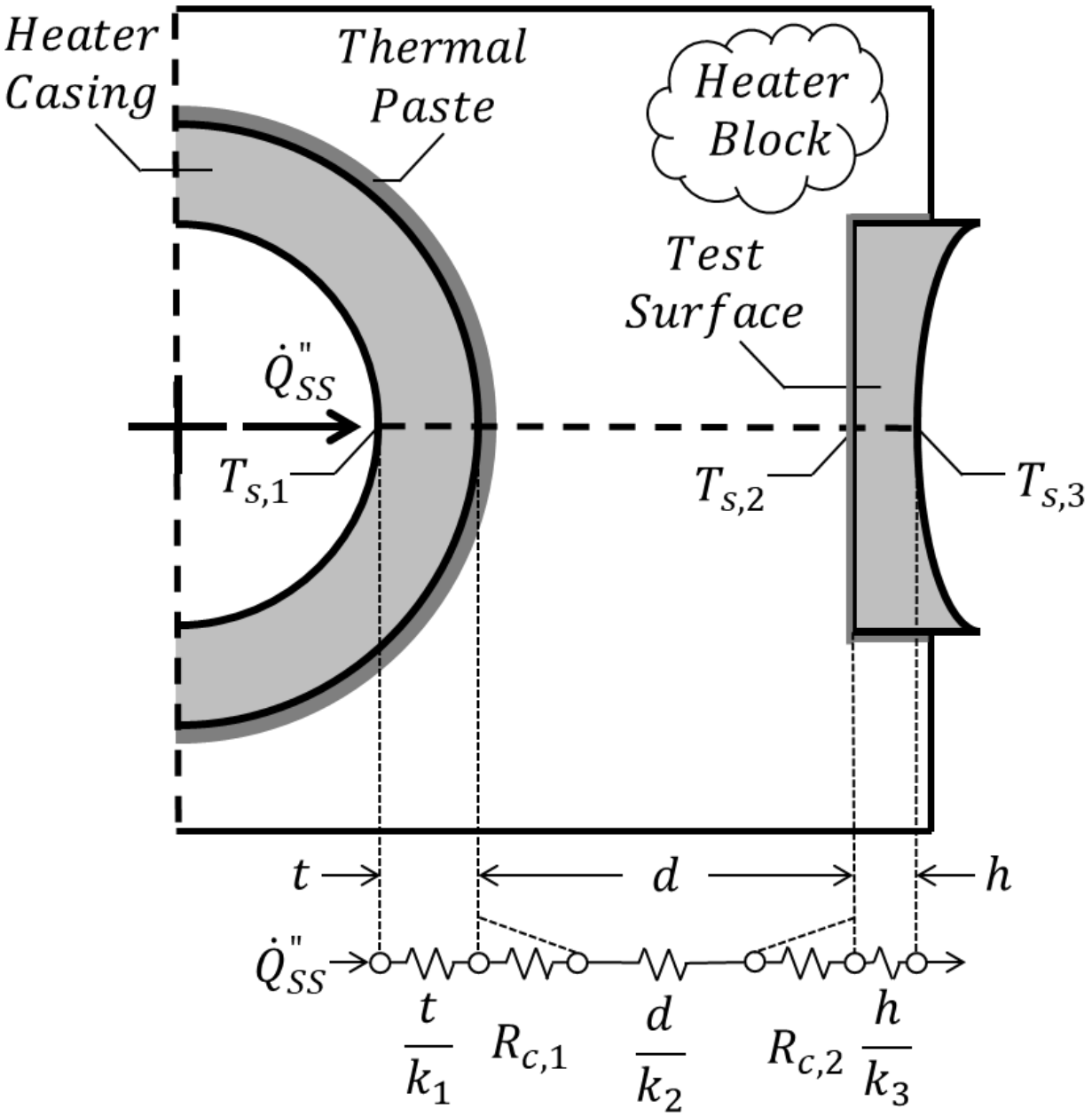

Figure 10. 1D schematic of heat transfer geometry. Dimensions in figure are not to scale.

The series of calibration data points previously presented (Fig. 7) includes simultaneous measurements of $T_{s,1}$, $T_{s,2}$, and $T_{s,3}$, such that the steady-state heat transfer rates can be computed and utilized to solve for the unknown contact resistance ($R_{c,2}$). The computed heat transfer rates are shown in Fig. 11 and correlated to the directly controlled internal surface temperature of the

resistance heater ($T_{s,1}$). A calibrated value computed from these data for the contact resistance is $R_{c,2}$~4.4 $\times 10^{-5}\, m^2 \cdot K/W$.

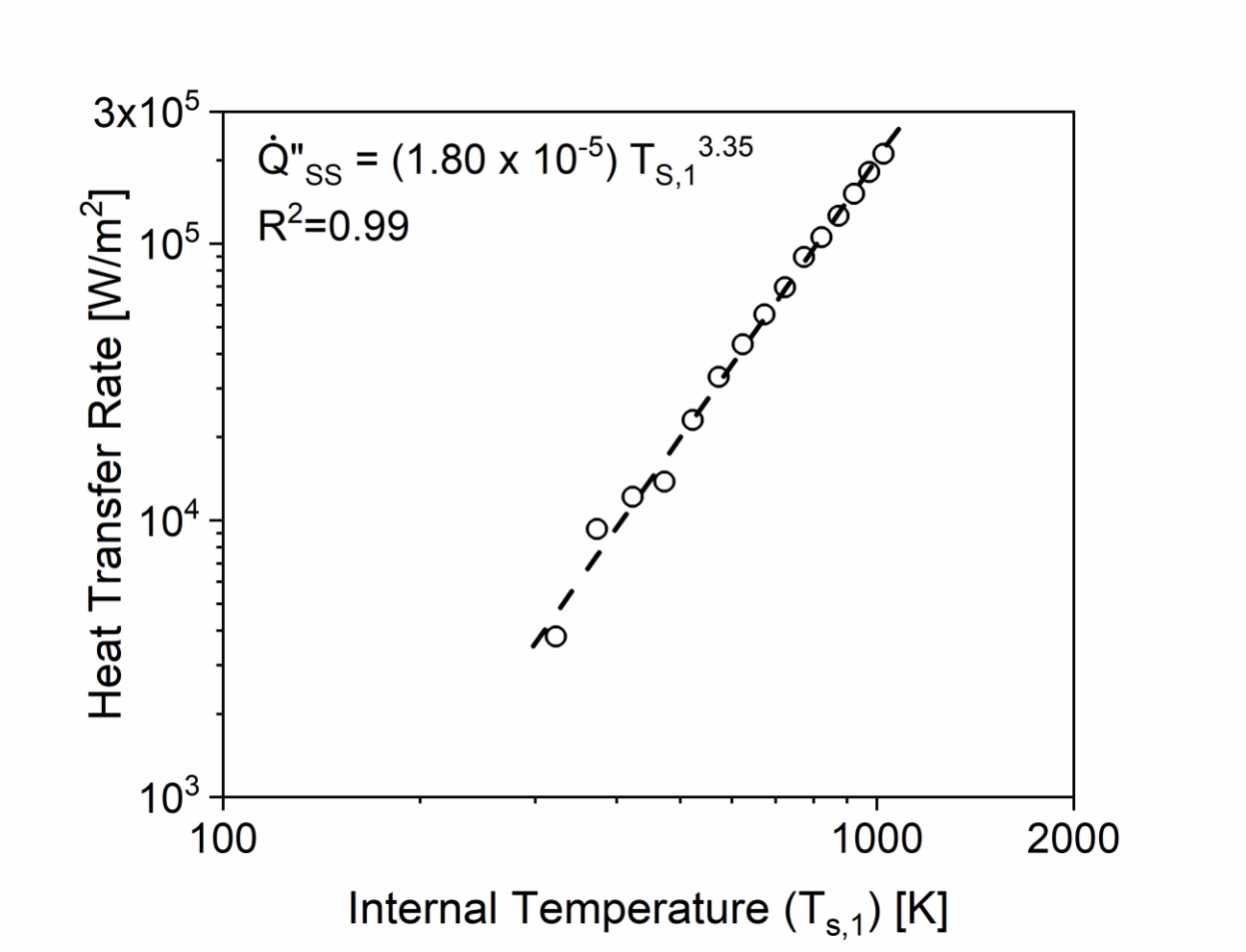

Figure 11. Rate of heat transfer vs internal set temperature.

The steady-state heat flux rate correlation (Fig. 11) and calibrated contact resistance value allow for complete one-dimensional modeling of the experiment with Eq. (1). It is worth noting that utilizing the heat transfer rate correlation for alternative test surface materials assumes that this rate is independent of the test surface material's thermal properties, which is valid given the small thickness/mass of the test surface in comparison to the thickness/mass of the SS block.

The developed model was compared to the calibration data. The prediction residuals are plotted against the measured surface temperature in Fig. 12, and statistical parameters are shown in Table 2. The greatest deviation from the predicted value is 8.52 K, but the average residual is 2.65 K.

Table 2: Temperature Uncertainties

Parameter	Value	Units
R^2	1.0000	-
$\lvert\Delta T\rvert_{max}$	8.52	K
	1.22	%
$\lvert\Delta T\rvert_{AVG}$	2.65	K
	0.40	%
ΔT_{AVG}	1.56	K
	0.26	%

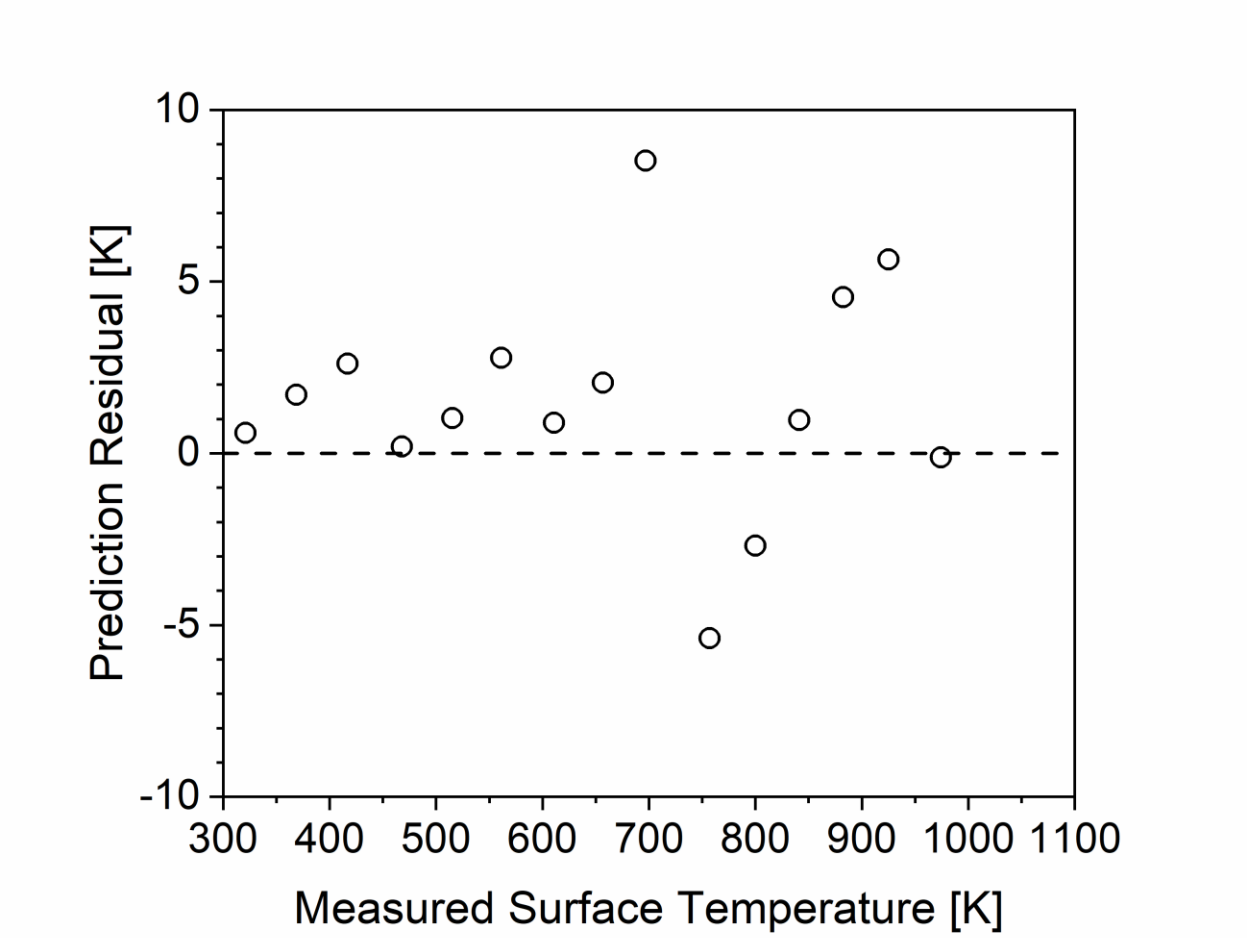

Figure 12. Prediction residuals vs measured surface temperatures. This data shows the uncertainty in temperature measurements. Most residuals are less than ± 3 K.

The model accurately captures the thermal behavior of the experiment and can be utilized to systematically study the effects of varying the test surface properties, i.e., thermal conductivity and contact resistance. Figure 13 illustrates the effects of varying these parameters over several orders of magnitude, where the baseline values were those utilized in the model formulation and calibration. The results illustrate that drastic changes in the relevant test surface properties are required to significantly affect the surface temperature. Large (several orders of magnitude) increases in the thermal conductivity or decreases in the contact resistance improve heat transfer to the test surface, but the maximum theoretical surface temperature is limited by the heater's

temperature, so that these changes do not yield significant effects. Similarly, significant decreases in thermal conductivity or increases in contact resistance are required before notable effects are observed. These observations indicate that the current calibration temperature curve can be utilized regardless of the test surface material, and that the system is tolerant to moderate changes in the test surface's contact resistance.

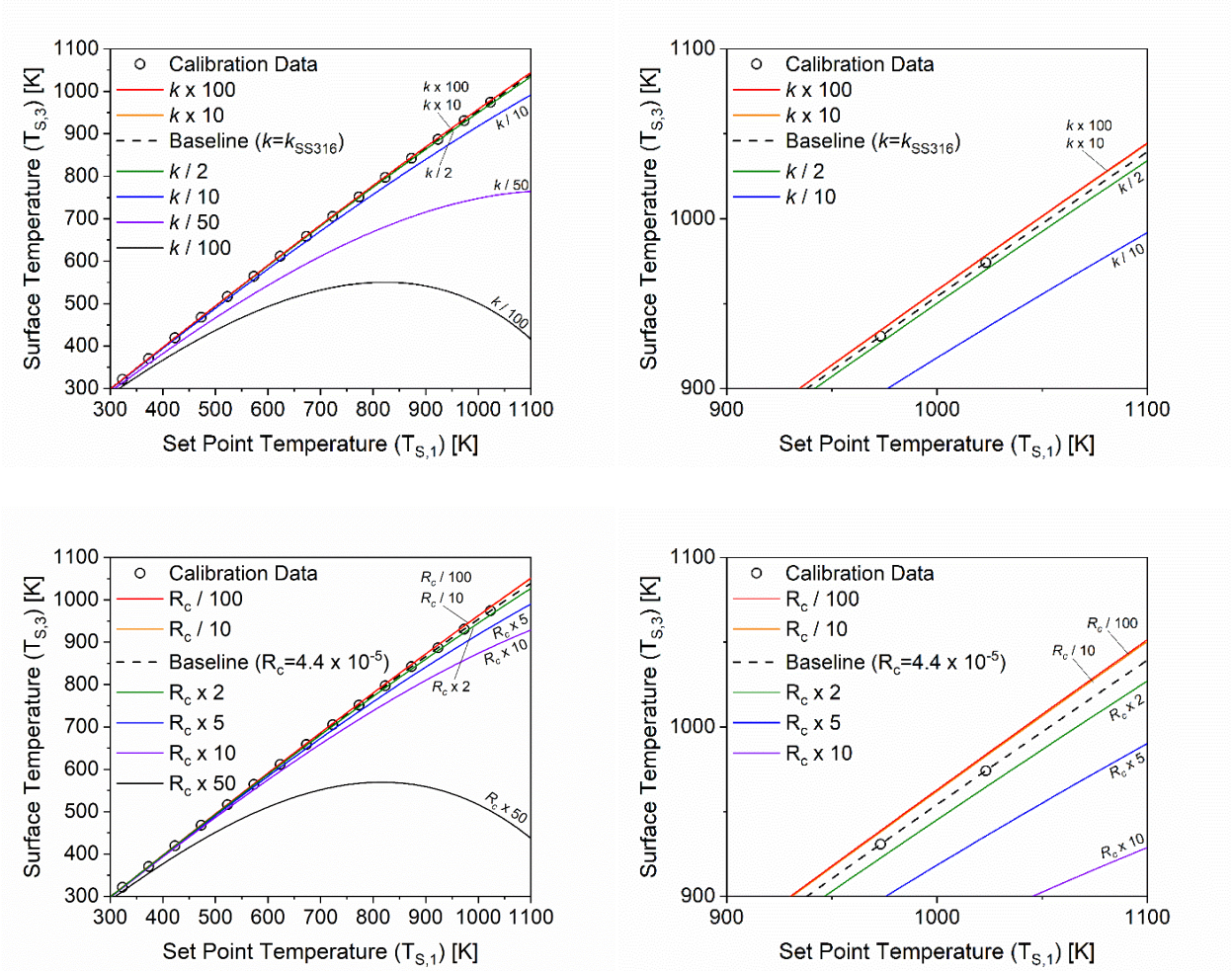

Figure 13: Parametric study results. Top Left: Thermal conductivity of the test surface is modified to see the effect on surface temperatures. Top Right: A zoomed in section of the top left plot shows minimal difference between surface temperatures for different thermal conductivities. Bottom Left: Contact resistance between the test surface and the SS block is modified to determine the effect on surface temperature. Bottom Right: A zoomed in section of bottom left plot shows the minimal temperature differences expected.

CHAPTER IV

HIGH-SPEED VIDEO ANALYSIS*

Fundamental HSI behavior can be gleaned from high-speed video analysis of these phenomena. A set of twenty oil droplet ignition tests were completed at identical conditions using the hot-surface experiment without the top layer of insulation and or air barriers, and a select number of tests are presented herein to describe key observations and general trends. Note that two test surfaces are visible in the images shown herein (Figs. 14-17), but only the rear surface was utilized in the current testing program. The droplets were always released onto the rear test surface, but the front test surface can be useful to compare with when attempting to visually differentiate the droplet from the rear test surface.

In general, a mild air current was observed traveling from right to left over the hot surface. The current was imperceptible to bare skin and was only recognized through analysis of the high-speed video. The air current carried the oil vapors such that ignition typically occurred to the left of the test surface, but not always. This observation highlights an important finding: in a seemingly quiescent environment, such as inside a controlled fume hood with vents turned off, there may exist some forced air currents that may influence the ignition behavior of liquid fuels. The high-speed video still frames shown herein should thus demonstrate the importance of incorporating air barriers around the hot surface when attempting to create quiescent conditions.

Figures 14-18 depict Mobil DTE 732 oil droplet ignition experiments at approximately 700 °C, but disparate behavior is observed on a test-by-test basis. In Fig. 14, ignition occurs off to the left side of the test surface, near the surface of the SS block, and then propagates around the edge

* Reprinted with permission from "High-Speed Video Analysis of Lubricating Oils Undergoing Hot-Surface Ignition" by David S. Teitge, James C. Thomas, and Eric L. Petersen, 2020. AIAA Propulsion and Energy Forum, Copyright 2020 by the authors.

of the test surface. This trend is seen in eight of the videos (40%) and may be caused by the geometry of the test surface. It does show that despite the transverse air current, fuel vapors are spreading out over the hot surface in all directions. The location of ignition is also of importance. As discussed earlier, the metal oxides on the hot surface act as catalysts. This catalytic nature and the potentially higher temperatures make the surface the most likely region for ignition, although this is not always the case. Figure 15 shows an ignition event that occurs above the surface but then propagates down and around the test surface. It also appears that there could be two separate ignition sites at 0.032 seconds, although the second ignition site may be derived from the first ignition event.

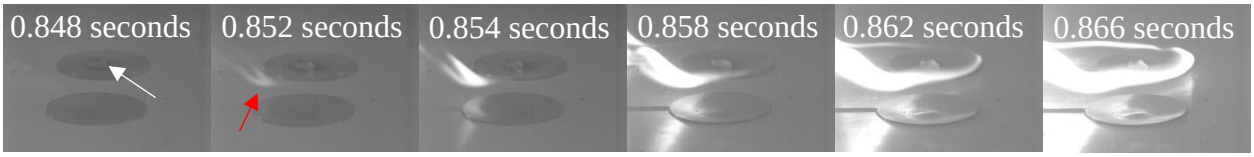

Figure 14. High-speed video of near surface ignition. The still frames show the ignition of the oil on the hot surface. The white arrow indicates the position of the oil droplet. The red arrow indicates the location of the first ignition spot. Reprinted with permission from [19].

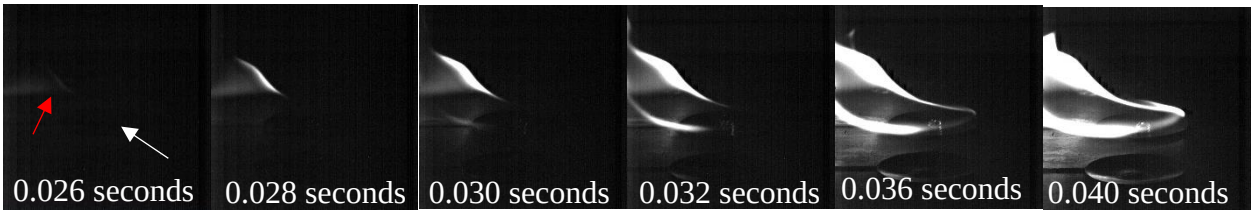

Figure 15. High-speed video of ignition of the surface. These still frames were taken with a smaller aperture and faster shutter to reveal more flame features. The same arrow convention used in Fig. 14 applies here. Reprinted with permission from [19].

The presence of separate ignition sites is possible and is not unexpected. In the droplet ignition experiment depicted in Fig. 16, four separate ignition sites are observed. The first one appears near the edge of the test surface, and then subsequently three more appear over the test surface itself. The first ignition site may have provided additional radiative heat input from the flame to the other sites to cause ignition, but all sites had the necessary stoichiometry for ignition. This observation likely implies that the combustible mixture ratios exist in many locations over the hot surface during the droplet evaporation process. If the hot, unreacted gas mixture receives the necessary heat input before natural convection and/or forced air currents displace them from the hot surface, then ignition can occur and spread to other areas where a combustible vapor mixture is present. The relative density of the fuel vapors, when compared to the density of the nearby air, may help keep the fuel vapors near the surface. Recalling the observed mild air current flowing from right to left over the plate, the three ignition locations over the test surface could be a region where fuel and air are mixing close to the necessary temperature.

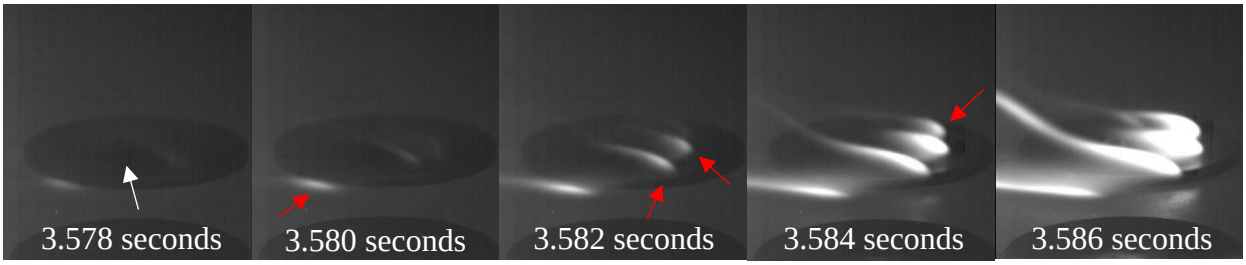

Figure 16. High-speed video showing multiple ignition regions. The stills showing the development of four ignition zones on and around the test surface. Reprinted with permission from [19].

In roughly half of the tests, the liquid droplet was observed to contain a bubble of evaporated, gaseous vapors constrained by the liquid's surface tension. The bubble would grow as liquid fuel continued to evaporate until the droplet 'popped' and released all the vapors rapidly, as seen in Fig. 17. This popping represents the greatest release of hot vapors to the surrounding air at one instant. In the tests conducted herein, the droplets generally had attached flames before popping occurred. Furthermore, one in five of these popping events is violent enough to eject some fluid, as can be seen in Fig. 18. This ejection of a small fireball provides an additional safety concern since the droplets already move freely due to the Leidenfrost effect. The ejection of flaming oil increases the chances of a fire spreading to surrounding areas.

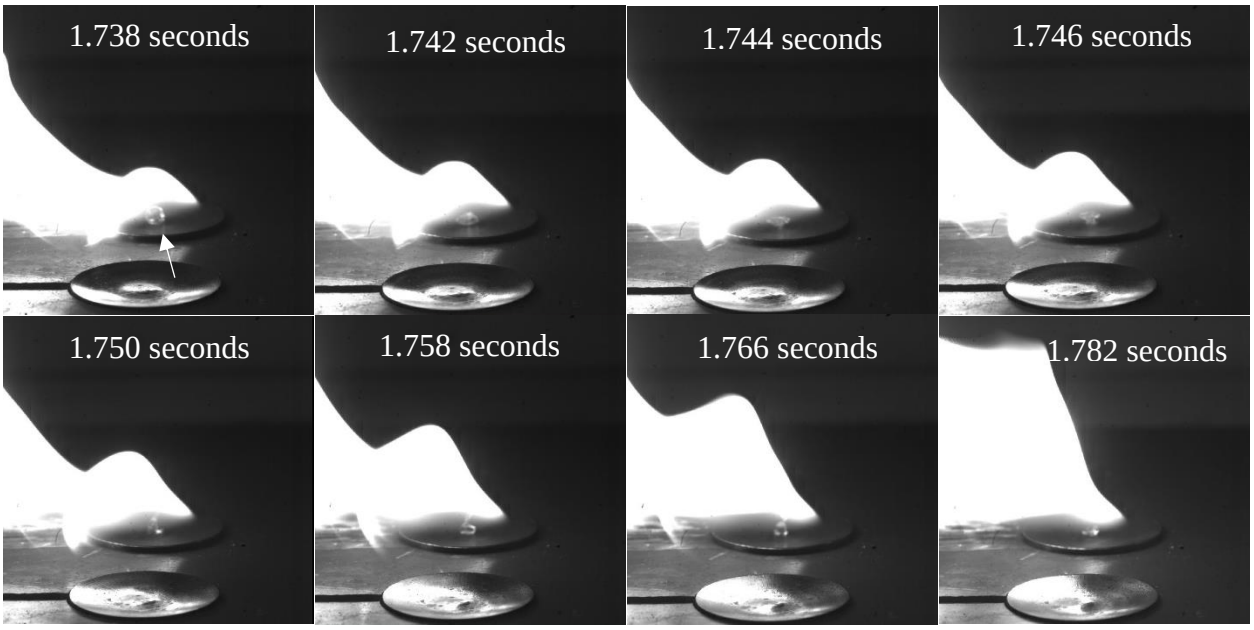

Figure 17. High-speed video stills of droplet popping. The popping droplet released vapors that had been trapped inside by surface tension. The droplet assumes many amorphous shapes before returning to a spherical shape. Reprinted with permission from [19].

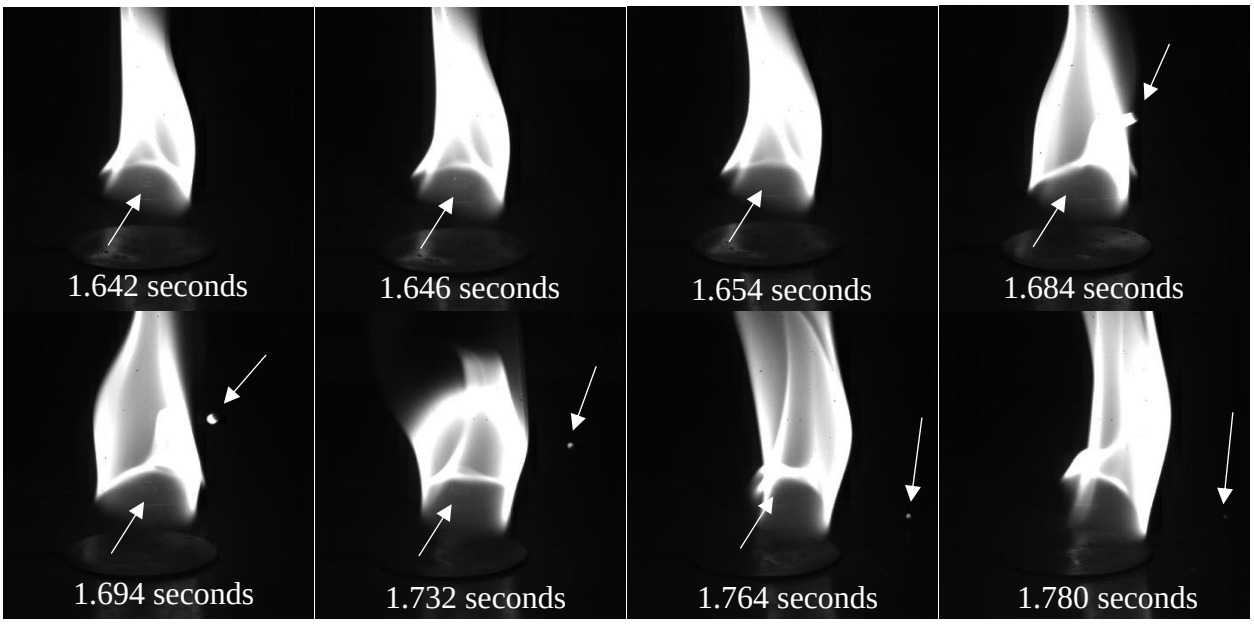

Figure 18. High-speed video stills of violent droplet popping. These images depict the droplet popping beginning around 1.646 seconds. Thirty-eight milliseconds later, part of the droplet is ejected from the top of the flame, depicted by the upper arrow. The ejected droplet evaporates and burns as it falls to the SS block where it bounces once before burning out. Reprinted with permission from [19].

A high-speed video test performed early in the project before the use of test surfaces is shown in Fig. 19. While the oil travels on the surface, the droplet does not visibly change in size until it suddenly pops (happens between first and second images in Fig. 19), releasing vapor that was trapped by surface tension. The liquid returns to a ball shape and begins traveling around the surface again without much delay. The vapor that was released by the pop is likely the greatest flux of fuel vapor to the surrounding hot air, making this event a common precursor to ignition of the oil (seen in the fourth image). In these images, it is unclear if the ignition origin is located behind the droplet and close to the surface or if it is in the space immediately above the droplet. Based on the other tests, this ignition was likely near the surface, but this is conjecture.

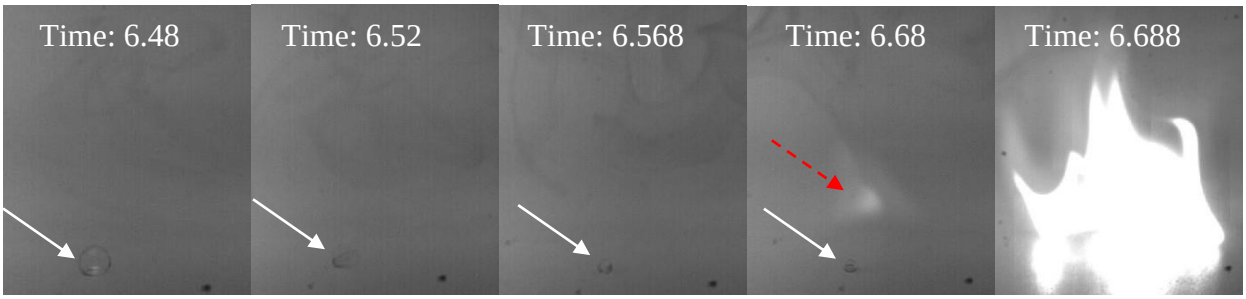

Figure 19. First generation high-speed video stills with ignition after pop. White arrows indicate the liquid droplet position, and the red dashed arrow indicates the origin of the flame. Reprinted with permission from [16].

CHAPTER V

IGNITION PROBABILITY DATA*

Although high-speed video is useful for fundamental phenomenological observations, the main interest of the experiments conducted herein was direct measurement of the temperatures where these fluids will ignite due to HSI. As discussed in Chapter II, HSI is a probabilistic event that is dependent on many environmental properties. Therefore, the temperature dependency of HSI for a fluid can be determined by holding all other relevant factors constant.

For all experiments completed using the current experimental setup, one drop was dispensed on a test surface at a time. After each droplet had been consumed, the fume hood vent was turned on for one minute, followed by one minute with the vent off before the next drop was dispensed. This procedure removes any combustion/decomposition products from the experiment's vicinity and allows for the test surface to return to steady state temperature. Ten total drops were tested on a single test surface before it was replaced with a new test surface. In general, an additional ten drops were tested at the same temperature, such that 20 total drops were tested at each temperature. It was observed in prior experiments that 20 drops per temperature were sufficient to determine the ignition probability at one temperature, and this observation was also documented in the literature discussed in Chapter II.

After the ignition probability was determined at one temperature, the temperature was incremented, and the process was repeated. This iterative process continued until HSI values ranging from 0% to 100% were gathered. This procedure yields a measurement resolution of ignition probability of 5% at each temperature; however, the stochastic nature of these phenomena

* Reprinted with permission from "Ignition Probability of Fuels and Oils Undergoing Hot-Surface Ignition" by David S. Teitge, James C. Thomas, and Eric L. Petersen, 2021. Central States Section of the Combustion Institute.

yield scatter that is on the order of ±10%, which is further discussed later. Implementing more drops per temperature could improve the ignition probability resolution, but with minimal gains considering the time it takes to collect the extra data and the repeatability of the data.

The ignition probability can be described with a logistic regression curve fit of the form:

$$P(I) = \frac{100}{1+\exp\left(-k*(T-T_{50})\right)} \tag{6}$$

where k and T_{50} are empirical constants that describe the ignition behavior of the fluid. The T_{50} coefficient corresponds to the temperature where 50% ignition probability is expected, and the k coefficient describes the rate of change of ignition probability with temperature.

The LTI and HTI are important markers for the ignition behavior of the liquid. The LTI represents the lowest temperature where ignition is recorded for the fluid. This lower bound is important information from a safety standpoint since it represents a threshold for the temperature of machinery surrounding the fluid. A safety factor equal to at least the temperature difference between surface temperature increments should be utilized for this value. The HTI represents the highest temperature without ignition. This is an important value for engineers designing propulsion or power generation systems that want to utilize HSI to their advantage. The ignition delay time for the fuel can also be critical for these systems, since the working fluids are generally not resting in a quiescent environment, such as the one emulated in the experiments conducted herein.

Representative HSI data and logistic regression curve fits are shown in Fig. 20 for two lubricating oils: Mobil DTE 732 and Chevron Regal R&O. The empirical coefficient and LTI/HTI data for these oils are provided in Table 3. Similar general HSI behavior and logistic empirical coefficients are observed for both lubricating oils. The minor difference in k coefficient falls within the statistical uncertainty of these coefficients (90% confidence interval).

Table 3. Lubricating oil ignition data. Reprinted with permission from [21].

Fluid	Mobil DTE 732	Chevron Regal R&O
k (1/°C)	0.038 ± 0.006	0.056 ± 0.008
T_{50} (°C)	573.2 ± 4.4	573.1 ± 3.2
LTI (°C)	510.0	519.7
HTI (°C)	615.9	626.8

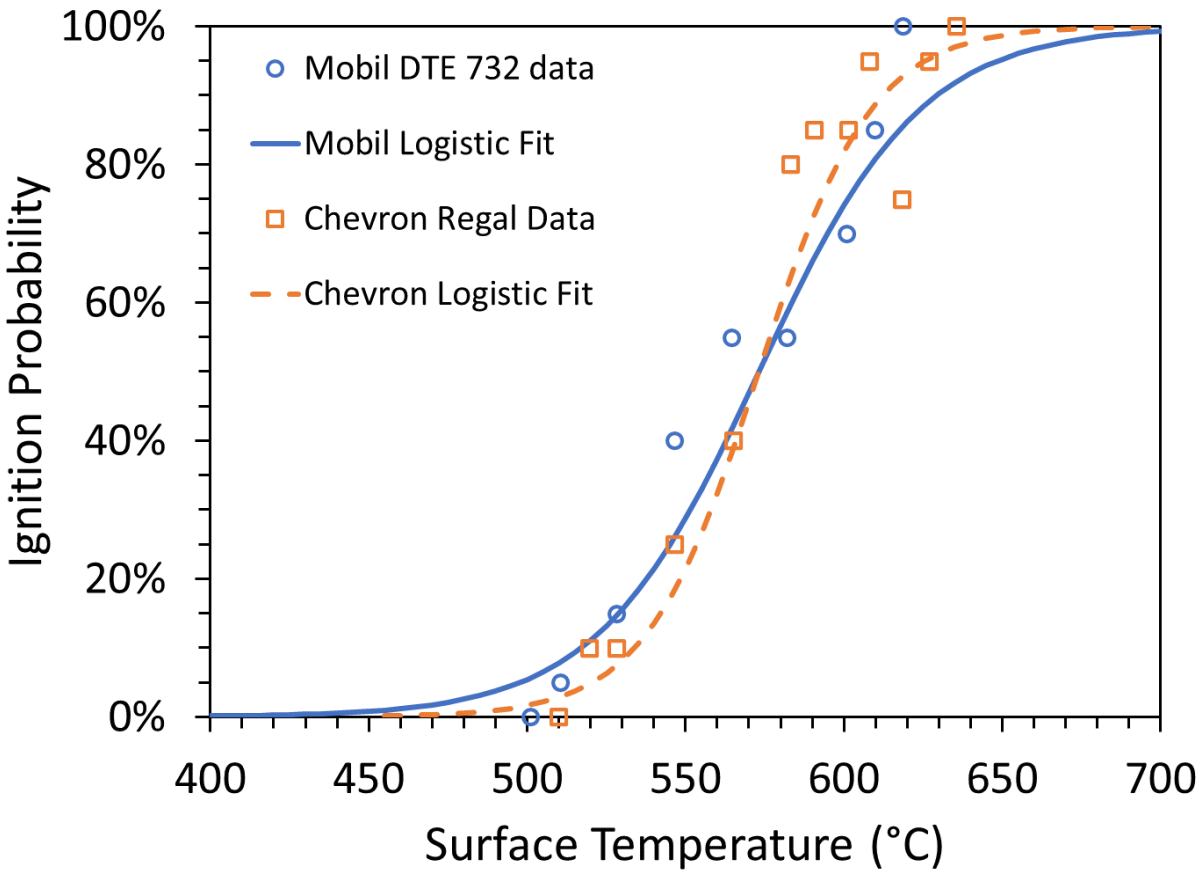

Figure 20. Lubricating oil ignition probability data. In the figure above, data for two lubricating oils with corresponding logistic regression curve fits are shown. Reprinted with permission from [21].

As expected, ignition probability generally increases with temperature. There are some isolated instances where an increase in temperature does not result in an increase in ignition probability. This counterintuitive result is potentially due to many factors influencing the ignition, which can be difficult to isolate, or the stochastic nature of HSI. Factors that are seemingly trivial, such as where the droplet hits the test surface, can affect if the liquid ignites or not, even if the droplet eventually reaches the center of the test surface. However, measured ignition probabilities that are outliers are generally easy to identify. For example, in Fig. 16, the Chevron data point around 620 °C seems significantly lower than the expected trend in comparison to the rest of the dataset. One set of 10 drops at that temperature had an ignition probability of 60%, while the other set had a probability of 90%. The more dissimilar the two results, the more likely one of those probabilities is incorrect. In this case, the 60% value is probably wrong, but this cannot be verified until the full ignition probability dataset has been collected.

In general, there is a lack of high-quality HSI data provided within the literature. For instance, there are no data provided within the literature for these lubricating oils, which make the datasets provided in Fig. 20 and Table 3 the first of their kind. This strong lack of comparable data within the literature makes it difficult to compare the current experiment to others with similar datasets. However, the author has conducted a series of experiments with ethanol and nitromethane to compare with data provided by Exponent, Inc. [11,6].

Prior to direct comparison of these data, the differences between Exponent's experiment and the current study should be considered. The biggest difference between these studies was the amount of fuel used per test. The current study used 20.5-µL drops, whereas the Exponent team utilized 250-µL sprays. The increased volume and spray injection of liquid is expected to make ignition more probable. The large number of droplets dispersed over the surface in this manner

potentially creates significantly more regions where the stoichiometry is prime for HSI. In addition, the exponent team generally placed a cover over the hot surface in between each test to raise the maximum surface temperature. This cover was abruptly removed before testing which potentially led to a transient thermophysical environment over the hot plate during HSI testing. This approach ultimately yields a less-controlled experiment. Furthermore, the Exponent team utilized a thermocouple welded atop of the hot surface, but far away from the center region to report the surface temperature. They defended this method by showing the temperature distribution over the hot plate with nine thermocouples, but only while the cover was on. The presented temperature distribution therein showed the hottest temperature was not in the center of their hot surface, and there was no notion of the temperatures on the surface after the cover had been removed. It appears the Exponent team utilized the cover method to overcome limitations in their electrical heaters to reach higher surface temperatures, but it ultimately yielded a significant reduction in control of the experiment.

The HSI data collected for ethanol in the current study and by Exponent [11] are compared in Fig. 21 and Table 4. It should be noted that no ignition was recorded for ethanol on the removeable test surfaces at any temperature in this experiment. All data recorded for ethanol in this study were collected by dropping the fluid on the hot surface recession where the embedded thermocouple is located. The resistance heaters for the current study have a maximum ‘infinite lifetime’ setpoint temperature of 760 °C, which does not produce hot enough surface temperatures to record 100% ignition probability with ethanol but does allow for collection of a range of ignition probabilities. Higher surface temperatures are achievable with the current system, but application of these temperatures risks the integrity of the resistance heaters.

The lack of ignition on the removable test surfaces is not solely because of surface temperature, since the temperature drop across the test surface is only a few degrees Celsius. Accordingly, this finding is almost certainly due to the catalytic nature of the oxidized surface on the ignition of ethanol. Based on pictures in Exponent's papers [6] and the description of their procedures, Exponent's surface is highly oxidized. This oxidation means the catalytic effects should also be seen in Exponent's data, possibly to an even greater extent since the surface used to collect the data for this study was covered by the removable test surface during most of its heated time. This could have prevented that surface from oxidizing at the same rate as the rest of the 304 SS block.

Even with all the differences between these experiments noted, the two data sets for ethanol HSI agree relatively well with each other. The larger fuel volumes and increased surface oxidation observed with Exponent's data was expected to yield a lower T_{50} coefficient than the current experiment, but this trend was not observed. This finding could potentially be explained by a combination of Exponent's testing procedures. No mention is made in Exponent's paper [11] to how the ignition surface was cleaned. This lack of documented cleaning may mean there was a buildup of combustion products or fuel residue on the surface that was altering the apparent ignition behavior. The higher ignition temperatures observed by Exponent may also be explained by the transient surface conditions before mentioned. The induced air flow from removing the cover and the temperature non-uniformities it causes on the surface could lower surface temperatures to a value below what their surface thermocouple measures. Ultimately, the two datasets are comparable, but more knowledge is required to fully rectify the minor differences.

Table 4. Ethanol ignition data comparison. Reprinted with permission from [21].

Reference	Current Study	Exponent [11]
k (1/°C)	0.1526 ± 0.0385	0.10878
T_{50} (°C)	680.1 ± 1.8	704.0
LTI (°C)	644.6	680
HTI (°C)	N/A	722

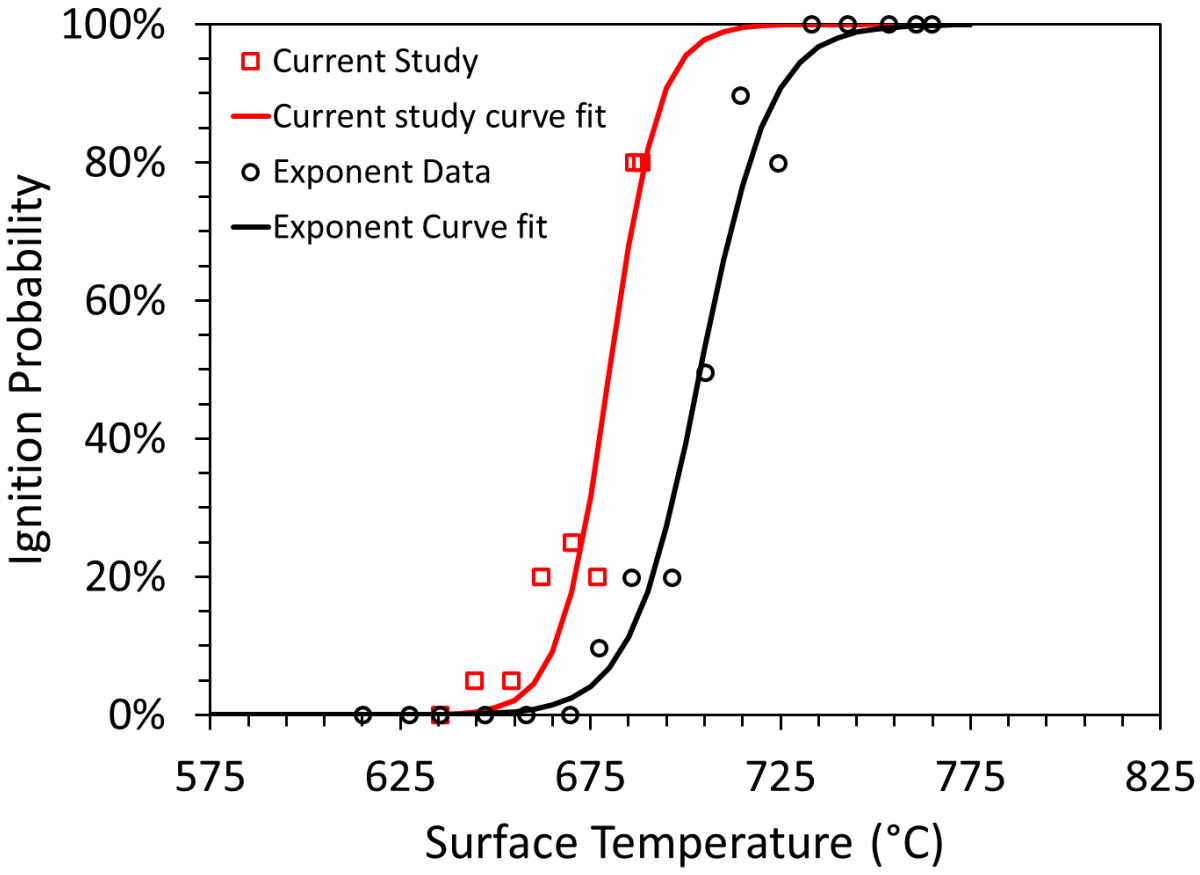

Figure 21. Ethanol ignition probability data. In the figure above is data for this study compared to data collected by Exponent [11]. Reprinted with permission from [21].

The HSI data collected for nitromethane in the current study and by Exponent [6] are compared in Fig. 22 and Table 5. Exponent generally utilized the same experiment and procedures for these tests as in their ethanol study [11], but in their nitromethane paper [6] there is mention of cleaning the surface between tests. Presumably before the heaters were turned on, the ignition surface was cleaned with steel wool and with ethanol. This process may have removed decomposition/combustion products or fuel residue, but it should have left most of the surface oxidation intact.

In comparison to the trends observed with ethanol, opposite trends were observed with nitromethane. More explicitly, data from Exponent [6] predicts much lower LTI temperatures than those observed in this study, as well as a shallower sloping ignition curve. The ~100 °C difference in these HSI data is, once again, likely related to the fluid volume and surface oxidation, since it is unreasonable to assume either group's surface temperature measurements are off by 100 °C.

These effects were further explored by altering the experimental procedures implemented herein. The baseline data from the current study is shown in Fig. 22 as 'Current study with test surface' and corresponds to 20.5-μL droplets on a removeable test surface. A set of data where the test surface is removed ('Current Study no test surface') was utilized to emulate an oxidized surface and a set of data with larger (90 μL) droplets ('Current Study 90 microliters') was utilized to explore the effect of droplet size. The no-test-surface data were recorded in the same way as the ethanol data were collected, e.g., droplets were dispensed directly onto the oxidized surface near the embedded thermocouple. As expected, this set of data is shifted to lower temperatures in comparison to the baseline data without surface oxidation. However, the shift in data is not large enough to fully rectify the differences between the data in the current study and those presented by Exponent [6].

The 90-µL data series was collected by dropping several droplets (5) out of a simple pipette onto the removable test surface, which yielded an average of 90-µL volumes. The average droplet volume was determined by weighing 50 drops from the simple pipette and dividing by the density of nitromethane. In general, the 5 drops all coalesced into one big drop on the test surface. One trend that was observed with the larger drops in comparison to the baseline 20.5-µL drops is that if ignition did not occur very shortly after the large volume hit the surface and coalesced, it did not ignite at all. This behavior contrasts with the 20.5-µL drops which could ignite any time during droplet evaporation. This observation suggests the large drops produce sufficient fuel vapor for ignition almost immediately, whereas the smaller drops must build up a vapor mass above the surface before the required HSI stoichiometry is satisfied. The larger-droplet data series is shifted to lower temperatures in comparison to the baseline data. However, once again, the shift in data is not large enough to fully rectify the differences between the data in the current study and those presented by Exponent [6]. These results ultimately indicate that both the combination of larger spray volumes and surface oxidation shift the HSI probability of nitromethane to lower temperatures. Furthermore, the combination of these effects may be large enough to explain the differences observed between the HSI data presented for nitromethane in the current study and by Exponent [6].

One trend that was observed in all the data collected in this study for nitromethane is the sharp jump in ignition probability, e.g., a large k term. Only 30 °C separates the 0% and 100% ignition points for nitromethane HSI for the baseline case in the current study, whereas Exponent [11] reports a 75 °C difference in their data. A large slope should be expected for fuels especially when compared to lubricating oils since fuels are designed for combustion, while oils are designed

to resist combustion (if it is even considered). This larger slope is seen in the order of magnitude difference in the k terms for the lubricating oils and nitromethane reported in this study.

Table 5. Nitromethane ignition data comparison. Reprinted with permission from [21].

Reference	Current Study	Exponent [11]
k (1/°C)	0.2168 ± 0.0269	0.0727
T_{50} (°C)	601.0 ± 0.7	503
LTI (°C)	587.3	462
HTI (°C)	615.2	515

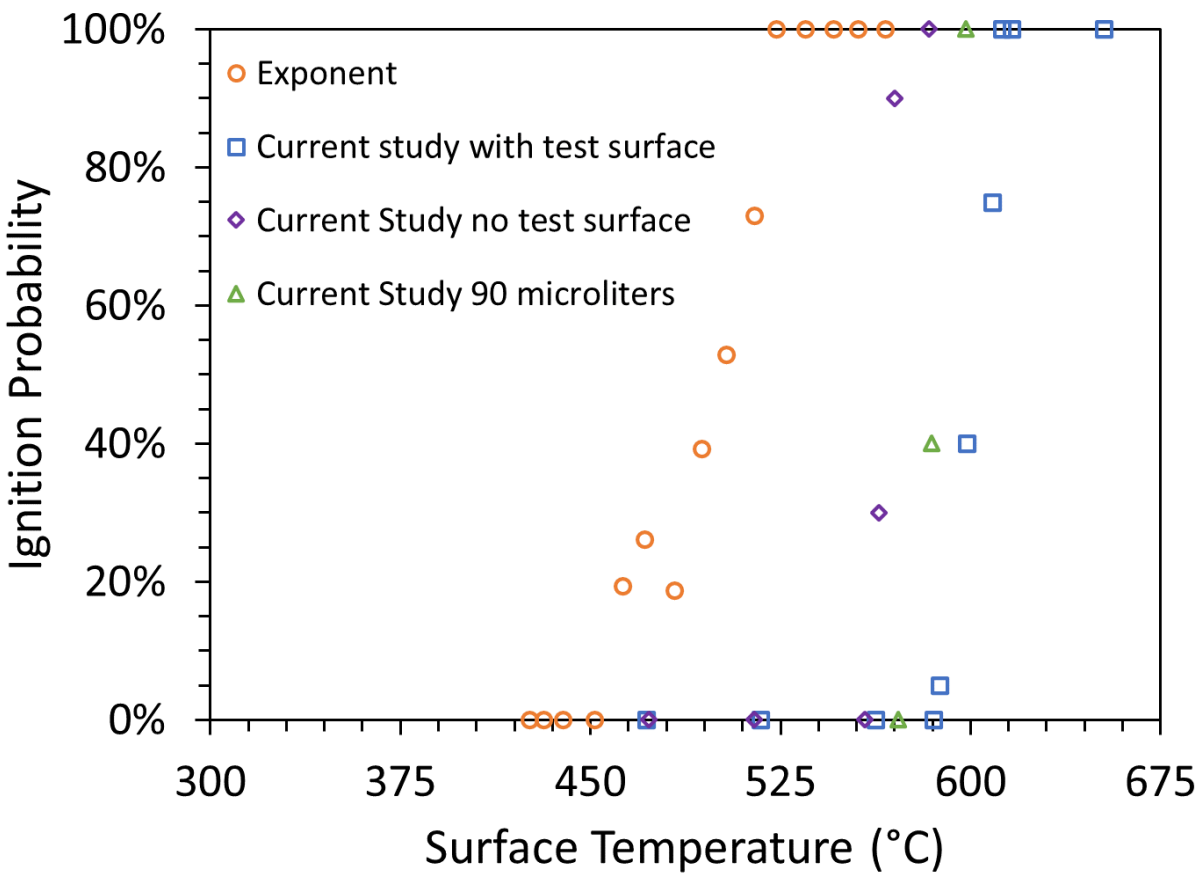

Figure 22. Nitromethane ignition probability data. HSI data for nitromethane collected in this study compared with HSI data collected by Exponent [6]. Two other methods were used to demonstrate their effects on HSI. These other methods' data should not be taken as standalone HSI data, but instead as a demonstration of general trends seen when experimental parameters are adjusted. Reprinted with permission from [21].

In summary, HSI probability is a concern of safety engineers or propulsion engineers working with flammable fluids, but HSI data are lacking in the literature. The data presented herein should serve as a guide to these engineers, but the variance in results between studies should be noted. Environmental parameters are very influential on HSI results. To know the HSI temperatures of a fluid with high certainty, experiments must be completed that closely mimic the conditions of interest.

CHAPTER VI

SUMMARY AND CONCLUSIONS

Summary

The HSI of flammable liquids is a complex problem affected by many environmental parameters. A well-controlled experiment was designed and optimized to control these parameters and measure HSI probability. A one-dimensional, steady-state heat transfer model was built to analyze the effects of alternative surface materials and contact resistances on the attainable surface temperatures. In addition to raw HSI probability data, the present experimental setup can be utilized to record high-speed video of these events, yielding unique insight into the physical behavior of the fluid during HSI events. Two lubricating oils and common fuels (ethanol and nitromethane) were tested and were shown to follow expected trends. Differences between data available in the literature and those recorded in the current study were discussed and potentially rectified by considering differences in experimental procedures.

Future Work

The HSI experiment presented herein is the product of several design iterations which has yielded one of the most well-controlled experiments for HSI in the current literature. Future work for the project includes studies on the ratio of exposed surface area to droplet volume to determine optimal values for these in this configuration of the experiment. With these values, a perfected experiment can be assembled with new heaters to allow testing at higher temperatures. This would allow for testing of fluids with higher LTIs, such as common jet fuels, along with any new fuels being currently developed.

REFERENCES

[1] Myronuk, D. J. (1980). Dynamic, “Hot Surface Ignition of Aircraft Fuels and Hydraulic Fluids,” SAN JOSE STATE UNIV CA.

[2] Babrauskas, V., “IGNITION OF GASES, VAPORS, AND LIQUIDS BY HOT SURFACES,” *Internal Symposium on Fire Investigation Science and Technology,* 2008.

[3] Byers, K., Epling, W., Cheuk, F. K., Kheireldin, M., and Weckman, B., “Evaluation of Automobile Fluid Ignition on Hot Surfaces,” *SAE Technical Paper Series,* 2007.

[4] Demetri, E. P. and White, B. F. (1985). “Development of a Model for Hot-Surface Ignition of Combustible Liquids,” ADVANCED MECHANICAL TECHNOLOGY INC NEWTON MA.

[5] Colwell, J. D. and Reza, A., “Hot Surface Ignition of Automotive and Aviation Fluids,” *Fire Technology*, Vol. 41, 2005, pp. 105–123.

[6] Davis, S., Kelly, S., and Somandepalli, V., “Hot Surface Ignition of Performance Fuels,” *Fire Technology,* Vol. 46, 2009, pp. 363–374.

[7] Ebersole, R. E., Matusz, L. C., Modi, M. S., and Orlando, R. E., “Hot Surface Ignition of Gasoline-Ethanol Fuel Mixtures,” *SAE International Journal of Engines,* vol. 2, 2009, pp. 1–8.

[8] Goyal, V., Benhidjeb-Carayon, A., Simmons, R., Meyer, S., and Gore, J. P., “Hot Surface Ignition Temperatures of Hydrocarbon Fuels,” 55th AIAA Aerospace Sciences Meeting, May 2017.

[9] ASTM E659-15, Standard Test Method for Autoignition Temperature of Chemicals, ASTM International, West Conshohocken, PA, 2015, www.astm.org

[10] Davis, S., Chavez, D., and Kytomaa, H., "Hot Surface Ignition of Flammable and Combustible Liquids," SAE Technical Paper Series, Mar. 2006.

[11] Somandepalli, V., Kelly, S., and Davis, S., "Hot Surface Ignition of Ethanol-blended Fuels and Biodiesel," SAE Technical Paper Series, 2008.

[12] ASTM D4206-96(2018), Standard Test Method for Sustained Burning of Liquid Mixtures Using the Small Scale Open-Cup Apparatus, ASTM International, West Conshohocken, PA, 2018, www.astm.org

[13] ASTM D92-18, Standard Test Method for Flash and Fire Points by Cleveland Open Cup Tester, ASTM International, West Conshohocken, PA, 2018, www.astm.org

[14] ASTM D1310-14, Standard Test Method for Flash Point and Fire Point of Liquids by Tag Open-Cup Apparatus, ASTM International, West Conshohocken, PA, 2014, www.astm.org

[15] Coward, H. F. and Guest, P. G., "Ignition of Natural Gas-Air Mixtures By Heated Metal Bars1," *Journal of the American Chemical Society*, Vol. 49, Oct. 1927, pp. 2479–2486.

[16] Teitge, D. S., Thomas, J. C., Sammet, T. E., Browne, Z. K., and Petersen, E. L., "Hot Surface Ignition Probability of Hydrocarbon Fuels and Oils," Central States Section of The Combustion Institute, May 2020.

[17] Tanabe, T., and Imoto, S., "Surface Oxidation of Type 316 Stainless Steel," *Transactions of the Japan Institute of Metals*, vol. 20, May 1979, pp. 507–515.

[18] Bennett, J. M., "Ignition of combustible fluids by heated surfaces," *Process Safety Progress*, vol. 20, Mar. 2001, pp. 29–36.

[19] Teitge, D., Thomas, J. C., & Petersen, E. L., "High-Speed Video Analysis of Lubricating Oils Undergoing Hot-Surface Ignition," *AIAA Propulsion and Energy 2020 Forum,* 2020 (p. 3887).

[20] Valencia, J. J. and Quested, P. N., "Thermophysical Properties," in *ASM Handbook Volume 15: Casting*, eds. Viswanathan, S., Apelian, D., Donahue, R. J., DasGupta, B., Gywn, M., Jorstad, J. L., Monroe, R. W., Sahoo, M., Prucha, T. E., and Twarog, D., ASM International, 2008. doi: 10.31399/asm.hb.v15.a0005240

[21] Teitge, D. S., Thomas, J. C., Petersen, E. L., "Ignition Probability of Fuels and Oils Undergoing Hot-Surface Ignition," 12th National Combustion Meeting, 2021.